UNIVERSIDADE FEDERAL DO RIO GRANDE DO NORTE CENTRO DE CIÊNCIAS EXATAS E DA TERRA PROGRAMA DE PÓS-GRADUAÇÃO EM GEODINÂMICA E GEOFÍSICA

DISSERTAÇÃO DE MESTRADO

CONTROLE ESTRATIGRÁFICO SOBRE A SILICIFICAÇÃO HIDROTERMAL NA FALHA AFONSO BEZERRA, BACIA POTIGUAR, BRASIL

Autor:
João Felipe de Sousa Neto

Orientador:
Prof. Dr. Moab Praxedes Gomes
Co-Orientador:
Prof. Dr. David Lino Vasconcelos

Dissertação n° 305/PPGG

Natal-RN
Julho de 2025

UNIVERSIDADE FEDERAL DO RIO GRANDE DO NORTE CENTRO DE CIÊNCIAS EXATAS E DA TERRA PROGRAMA DE PÓS-GRADUAÇÃO EM GEODINÂMICA E GEOFÍSICA

DISSERTAÇÃO DE MESTRADO

João Felipe de Sousa Neto

CONTROLE ESTRATIGRÁFICO SOBRE A SILICIFICAÇÃO HIDROTERMAL NA FALHA AFONSO BEZERRA, BACIA POTIGUAR, BRASIL

Dissertação apresentada em 28 de Julho de 2025 ao Programa de Pós-Graduação em Geodinâmica e Geofísica (PPGG) da Universidade Federal do Rio Grande do Norte (UFRN) como requisito à obtenção do Título de Mestre em Geodinâmica e Geofísica, com área de concentração em Geodinâmica.

Orientador:
Prof. Dr. Moab Praxedes Gomes

Co-Orientador:
Prof. Dr. David Lino Vasconcelos

Natal-RN
Julho de 2025

UNIVERSIDADE FEDERAL DO RIO GRANDE DO NORTE CENTRO DE CIÊNCIAS EXATAS E DA TERRA PROGRAMA DE PÓS-GRADUAÇÃO EM GEODINÂMICA E GEOFÍSICA

DISSERTAÇÃO DE MESTRADO

CONTROLE ESTRATIGRÁFICO SOBRE A SILICIFICAÇÃO HIDROTERMAL NA FALHA AFONSO BEZERRA, BACIA POTIGUAR, BRASIL

João Felipe de Sousa Neto

COMISSÃO EXAMINADORA:

Moab Praxedes Gomes (PPGG/UFRN)

David Lino Vasconcelos (LAPEP/UFCG)

José Antônio Barbosa (DGEOL/UFPE)

Pedro Xavier Neto

Natal-RN
Julho de 2025

Universidade Federal do Rio Grande do Norte - UFRN
Sistema de Bibliotecas - SISBI
Catalogação de Publicação na Fonte. UFRN - Biblioteca Setorial Prof. Ronaldo Xavier de Arruda - CCET

Sousa Neto, João Felipe de.
Controle estratigráfico sobre a silicificação hidrotermal na falha Afonso Bezerra, Bacia Potiguar, Brasil / João Felipe de Sousa Neto. - 2025.
90 f.: il.

Dissertação (mestrado) - Universidade Federal do Rio Grande do Norte, Centro de Ciências Exatas e da Terra, Programa de Pós-Graduação em Geodinâmica e Geofísica. Natal, RN, 2025.
Orientação: Prof. Dr. Moab Praxedes Gomes.
Coorientação: Prof. Dr. David Lino Vasconcelos.

1. Atributo sísmico - Dissertação. 2. Escape fluido - Dissertação. 3. Silicificação - Dissertação. 4. Vents hidrotermal - Dissertação. I. Gomes, Moab Praxedes. II. Vasconcelos, David Lino. III. Título.

RN/UF/CCET CDU 550.34.06(043.3)

Elaborado por Joseneide Ferreira Dantas - CRB-15/324

Agradecimentos

À Universidade Federal do Rio Grande do Norte (UFRN) e ao Programa de Pós-Graduação em Geodinâmica e Geofísica (PPGG), pelos apoios institucionais, infraestrutura acadêmica e formação científica.

À Fundação Norte-Rio-Grandense de Pesquisa e Cultura (FUNPEC), à Shell Brasil e à Schlumberger, pelo suporte técnico e institucional. Agradeço especialmente à Shell Brasil pelo financiamento do projeto Porocarste – Fase II: Processos e Caracterização das Rotas de Fluxo de Fluidos em Reservatórios Carstificados, Fraturados e Silicificados do Pré-Sal, no qual esta pesquisa está inserida. À Schlumberger, pela cessão da licença educacional do software Petrel®, essencial na etapa de modelagem e interpretação sísmica.

Ao Professor Dr. Francisco Hilário Rego Bezerra, coordenador do projeto Porocarste – Fase II, pela liderança e pela confiança em permitir minha integração à equipe do projeto.

Ao meu orientador, Professor Dr. Moab Praxedes Gomes, pela orientação técnica, incentivo e condução científica ao longo do mestrado. Ao meu coorientador, Professor Dr. David Lino Vasconcelos, pelas contribuições metodológicas e apoio contínuo ao desenvolvimento desta pesquisa.

Agradeço aos Professores Dr. Pedro Xavier Neto e Dr. José Antonio Barbosa, por gentilmente aceitarem compor a banca examinadora.

A todos os professores, técnicos e funcionários do PPGG/UFRN, pela colaboração na minha trajetória acadêmica. Aos colegas de pós-graduação que dividiram experiências ao longo desta jornada, especialmente Lorenna Sávilla, Luiza Cavalcante, Cayo Pontes, Aline Tavares e Michel Câmara.

À minha esposa, à minha filha e aos meus pais, pela paciência, apoio incondicional e incentivo nos momentos mais desafiadores.

Aos amigos e demais pessoas que, direta ou indiretamente, contribuíram com este trabalho, o meu sincero agradecimento.

Resumo

A silicificação hidrotermal exerce um impacto significativo nas propriedades petrofísicas das rochas-reservatório. Os principais controles sobre os fluidos ricos em sílica são as falhas, suas respectivas zonas de dano e as variações na litologia hospedeira. No entanto, embora a influência da litologia hospedeira na silicificação seja parcialmente compreendida, estudos adicionais são necessários para esclarecer seu papel e seu impacto espacial. Neste estudo, as sequências cretáceas da bacia Potiguar, compostas pelos arenitos da Formação Açu, pelos calcários da Formação Jandaíra e pelas rochas cristalinas do embasamento neoproterozoico, são atravessadas pelo Sistema de Falhas Afonso Bezerra, onde ocorrem registros significativos de silicificação hidrotermal, desde o embasamento até a superfície. Foram utilizados dados sísmicos, integrados a dados de poços, com aplicação de atributos sísmicos para aprimorar a visualização e o mapeamento das unidades estratigráficas , bem como da geometria da silicificação hidrotermal. Foi realizada uma análise estatística espacial do corpo silicificado, com o objetivo de avaliar a relação entre a silicificação e a estratigrafia. Os resultados revelaram que os corpos silicificados se concentram ao longo do traçado da Falha Afonso Bezerra, que aparenta ser o principal conduto responsável pela ascensão dos fluidos hidrotermais. As variações de espessura e as mudanças na forma da zona silicificada estão associadas às diferenças litológicas. As rochas carbonáticas apresentam silicificação extensa, associada a volumes mais amplos de rochas afetadas, enquanto as rochas siliciclásticas exibem silicificação mais estreita e menos disseminada. No embasamento cristalino, a silicificação está restrita às zonas de falha. Essa distribuição espacial evidencia o controle primário da tectônica e da litologia hospedeira sobre o fluxo de fluidos hidrotermais, contribuindo para um melhor entendimento da compartimentação da silicificação hidrotermal.

Palavras-chave: Atributo sísmico; Escape fluido; Silicificação; Vents hidrotermal.

Abstract

Hydrothermal silicification has a significant impact on petrophysical properties of reservoir rocks. The main constraints on silica-rich fluids are the faults, their damage zones, and variations in the host lithology. However, although the influence of host lithology on silicification is partially understood, further studies are required to clarify its role and spatial impact. In this study, the Cretaceous sequences of the Potiguar Basin, comprising the sandstones of the Açu Formation and the limestones of the Jandaíra Formation, as well as the crystalline rocks of the Neoproterozoic basement, are crosscut by the Afonso Bezerra Fault System, where significant occurrences of hydrothermal silicification are observed from the basement to the surface. This study employed seismic data, along with well data, and applied seismic attributes to enhance the visualization and mapping of stratigraphic units and the geometry of the hydrothermal silicification. A statistical spatial analysis of the silicified body was conducted to assess the relationship between silicification and stratigraphy. The results revealed that silicified body concentrate along the strike of the Afonso Bezerra Fault, which appears to be the main conduit controlling the uprise of hydrothermal fluids. Width variations and shape changes of the silicified zone connected to the variations of lithology. Carbonate rocks exhibit extensive silicification associated with wider volumes of affected rocks, whereas siliciclastic rocks show narrower and less pervasive silicification. In the crystalline basement, silicification is confined to fault zones. This spatial distribution evidences the primary control of tectonics and host lithology on hydrothermal fluid flow, thereby enhancing our understanding of hydrothermal silicification compartmentalization.

Keywords: Seismic attributes; Fluid escape; Silicification; Vents hidrotermal.

Lista de Figuras e Tabelas

Índice da dissertação

Capítulo 1 – Introdução

1. INTRODUÇÃO

Esta dissertação está vinculada ao Programa de Pós-Graduação em Geodinâmica e Geofísica da Universidade Federal do Rio Grande do Norte (PPGG/UFRN), como parte do projeto Porocarste – Fase II, que tem como foco a investigação de processos relacionados ao fluxo de fluidos em reservatórios carstificados, fraturados e afetados por silicificação.

A silicificação hidrotermal corresponde a um processo pós-diagenético responsável por modificar substancialmente as propriedades petrofísicas das rochas hospedeiras, como porosidade e permeabilidade. Do ponto de vista hidrodinâmico, fluidos ascendentes enriquecidos em sílica tendem a migrar por falhas profundas e fraturas, estabelecendo rotas com elevada condutividade, que tanto favorecem a migração de fluidos quanto formam barreiras de baixa permeabilidade. Esse contraste influencia diretamente a compartimentação interna dos reservatórios. A depender da litologia hospedeira e da intensidade do processo, a precipitação de sílica pode atuar tanto na ampliação quanto na restrição da conectividade hidráulica (Bjorlykke and Egeberg, 1993; Ngwenya et al., 2000; Palhano et al., 2023; Klimchouk, 2017; Rocha et al., 2025).

A Bacia Potiguar, situada na margem equatorial nordeste do Brasil, oferece condições geológicas favoráveis para a investigação da silicificação hidrotermal. O Sistema de Falhas Afonso Bezerra (SFAB), que apresenta caráter predominantemente normal e foi posteriormente reativado com movimentações transcorrentes, corta diferentes litologias, incluindo o embasamento cristalino, as unidades siliciclásticas da Formação Açu e os carbonatos da Formação Jandaíra. Essas unidades revelam evidências significativas de silicificação associadas à migração de fluidos canalizada por estruturas tectônicas (Bezerra et al., 2009; Menezes et al., 2019; Bezerra et al., 2021).

Este trabalho visa analisar a relação entre a largura de um corpo geológico e a litologia hospedeira, bem como a influência estrutural exercida pelo SFAB. Para atingir esse objetivo, foram utilizados dados sísmicos 2D e 3D, processados com o filtro de ganho equalizador, conhecido como controle automático de ganho (AGC), e com o atributo de Variância, permitiram realçar descontinuidades sísmicas, condutos verticais e padrões geométricos internos relacionados à silicificação. Complementarmente, análises estatísticas foram realizadas a fim de quantificar a variação de espessura do corpo geológico e examinar possíveis correlações com a orientação estrutural (Maestrelli et al., 2017; Chen et al., 2021; Oliveira et al., 2023).

Este trabalho analisa como a largura de um corpo geológico na Bacia Potiguar, localizada no nordeste do Brasil (Fig. 1), está relacionada às litologias hospedeiras e às estruturas tectônicas. As principais questões que orientam a investigação são:

(i) Como as diferentes litologias (unidades cristalinas, siliciclásticas e carbonáticas) afetam a largura do corpo silicificado?

(ii) A transição entre essas unidades influencia a largura do corpo geológico?

(iii) Qual é o efeito das falhas sobre a largura da silicificação?

(iv) Os condutos hidrotermais apresentam heterogeneidades internas, nas quais porções da rocha hospedeira permanecem não afetadas pela silicificação ou são apenas parcialmente modificadas, sugerindo que a silicificação é seletiva e não pervade completamente a geometria do conduto?

A abordagem adotada integra dados sísmicos com o AGC e Variância, a fim de mapear zonas silicificadas e avaliar seus controles litológicos e estruturais. Um foco especial é dado à influência do Sistema de Falhas Afonso Bezerra (SFAB) sobre a forma e a distribuição espacial do corpo geológico analisado.

Os resultados obtidos contribuem para ampliar a compreensão do impacto da silicificação hidrotermal em distintos tipos de rocha, oferecendo subsídios importantes para a construção de modelos geológicos mais realistas e para a melhoria na previsão da qualidade dos reservatórios em contextos tectonicamente ativos.

Capítulo 2 - Fundamentação Teórica

2. FUNDAMENTAÇÃO TEÓRICA

2.1 Silicificação Hidrotermal

A silicificação hidrotermal é um processo pós-diagenético que altera significativamente as propriedades petrofísicas das litologias hospedeiras, especialmente a porosidade e a permeabilidade (Bjorlykke and Egeberg, 1993; Ngwenya et al., 2000; Palhano et al., 2023). Do ponto de vista hidrodinâmico, os fluidos ascendentes ricos em sílica migram por falhas profundas e fraturas, formando caminhos de alta condutividade que facilitam a migração, ao mesmo tempo em que promovem a precipitação de sílica e criam barreiras de baixa permeabilidade, fundamentais para a compartimentação dos reservatórios (Klimchouk, 2017; Rocha et al., 2025).

Esse processo ocorre em resposta a mudanças físico-químicas, como variações de temperatura, pressão ou pH, afetando tanto unidades sedimentares quanto o embasamento cristalino. A silicificação hidrotermal já foi registrada em diversas bacias sedimentares, como na Bacia Potiguar (Menezes et al., 2019), Bacia do Rio do Peixe (Palhano et al., 2023; Maciel et al., 2024; Rocha et al., 2025), Bacia de Thrace (Berio et al., 2025a, b), Bacia de Tarim (Lu et al., 2017; You et al., 2018), Bacia de Qiongdongnan (Chen et al., 2021) e nos sistemas carbonáticos do Pré-Sal brasileiro (Lima et al., 2019, 2020; Fernandez-Ibanez et al., 2022; Strugale et al., 2024; Corrêa et al., 2025).

A espessura e a geometria dos corpos silicificados apresentam variação lateral e vertical, sob controle combinado da estratigrafia e das estruturas tectônicas (Souza et al., 2021). Camadas mais porosas favorecem a migração ascendente dos fluidos hidrotermais, enquanto unidades com menor permeabilidade atuam como barreiras ao fluxo (Souza et al., 2021; Palhano et al., 2023). Além disso, a heterogeneidade estrutural exerce influência direta na conectividade entre compartimentos e na formação de caminhos preferenciais de fluxo (La Bruna et al., 2021; Corrêa et al., 2025; Rocha et al., 2025).

Em unidades carbonáticas, como a Formação Jandaíra, a substituição mineral pode gerar porosidade secundária, incluindo vugs e fraturas interconectadas, aumentando a permeabilidade e criando zonas de alta conectividade hidráulica (Fernandez-Ibanez et al., 2022; Basso et al., 2023; Corrêa et al., 2025; Bezerra et al., 2021). Já em rochas siliciclásticas, como os arenitos da Formação Açu, a precipitação de sílica tende a preencher os poros, reduzindo a permeabilidade, favorecendo a compactação mecânica e a formação de barreiras internas ao fluxo (Palhano et al., 2023; Berio et al., 2025a, b).

No embasamento cristalino, a silicificação é restrita a zonas de falhas e fraturas, onde a circulação de fluidos modula a condutividade hidráulica. Esse processo resulta em uma distribuição heterogênea, marcada por zonas intensamente cimentadas e impermeáveis, intercaladas com fraturas porosas do tipo vuggy, formadas por múltiplos episódios de silicificação estática e dinâmica (Menezes et al., 2019; Bezerra et al., 2021; Maciel et al., 2024).

2.2 Contexto Geológico

A Bacia Potiguar localiza-se na porção oriental da Margem Equatorial Brasileira, abrangendo uma área de aproximadamente 60.000 km². Sua configuração estrutural foi estabelecida a partir do rifteamento ocorrido no Neocomiano e está marcada por falhas normais, com direção predominante NE–SW, e por estruturas reativadas NW–SE, como o Sistema de Falhas Afonso Bezerra (SFAB). Essa rede de falhas teve papel fundamental na compartimentação da bacia e na condução de fluidos hidrotermais ao longo de suas fases tectônicas (Matos, 1992; De Castro et al., 2012; Bezerra et al., 2006; Menezes et al., 2019).

As principais unidades geológicas envolvidas no presente estudo são o embasamento cristalino e as formações Alagamar, Açu e Jandaíra, que registram diferentes respostas à silicificação hidrotermal. A influência combinada da litologia hospedeira e da estrutura tectônica define os padrões de alteração e a conectividade dos corpos silicificados.

A descrição detalhada das formações mapeadas, dos horizontes sísmicos e das características estruturais será apresentada no item 4 – Resultados desta dissertação.

Capítulo 3 – Dados e Metodologia

3. DADOS E METODOLOGIA

Este trabalho utilizou dados sísmicos 2D, volume sísmico 3D e perfis de poços fornecidos pela Agência Nacional do Petróleo, Gás Natural e Biocombustíveis (ANP), acessados via plataforma REATE, em cooperação com o Serviço Geológico do Brasil (SGB). Os dados são públicos e foram utilizados exclusivamente para fins científicos, conforme os termos de uso da ANP.

As seções sísmicas 2D representam cortes verticais obtidos ao longo de linhas de aquisição, úteis para mapeamentos regionais. Já os dados 3D permitem a construção de volumes contínuos da subsuperfície, com maior resolução lateral e possibilidade de interpretação em múltiplas direções.

A interpretação foi realizada no software Petrel®, da Schlumberger, utilizando fluxo metodológico padronizado na indústria: importação e calibração com dados de poço, identificação de horizontes e falhas, e aplicação de atributos sísmicos. Foram empregados dois recursos principais: o filtro de ganho equalizador AGC (Automatic Gain Control), para balancear os níveis de amplitude ao longo das seções, e o atributo de Variância, voltado à realce de descontinuidades estruturais.

Essa abordagem permitiu a delimitação do arcabouço estrutural e das relações estratigráficas da área de estudo, com base na integração entre dados sísmicos e perfis de poço.

3.1 – Dados Sísmicos 2D e 3D

A sísmica de reflexão é a principal técnica geofísica aplicada ao imageamento da subsuperfície, podendo ser realizada em duas (2D) ou três dimensões (3D), conforme o objetivo exploratório e o nível de detalhamento desejado. Na aquisição 2D, os dados são registrados ao longo de uma única linha de perfil, gerando seções verticais que representam cortes bidimensionais da subsuperfície (Yilmaz, 2001). Já os dados 3D são adquiridos em uma malha regular de fontes e receptores, permitindo a reconstrução volumétrica e a análise contínua em todas as direções (Chopra & Marfurt, 2007).

A sísmica 2D apresenta menor custo e é útil para levantamentos regionais e fases iniciais de exploração. Contudo, sua resolução lateral é limitada, e eventos estruturais inclinados ou fora do plano podem ser mal interpretados (Nanda, 2016). Em contrapartida, os dados 3D oferecem imagens mais confiáveis e detalhadas da geometria dos estratos e falhas, além de permitir a geração de fatias horizontais (time-slice) e visualizações cruzadas (inline e crossline), essenciais para a caracterização de reservatórios (Nanda, 2016; Chopra & Marfurt, 2007; Yilmaz, 2001).

Comparativamente, a sísmica 3D possui maior capacidade de modelar estruturas complexas, como condutos verticais, zonas de escape de fluidos e compartimentos estruturais, sendo indicada para aplicações em ambientes tectonicamente ativos. Apesar disso, seu custo elevado e a alta demanda computacional são fatores limitantes em algumas regiões (Chopra & Marfurt, 2007; Yilmaz, 2001).

Por fim, a integração entre dados 2D e 3D, aliada a atributos como Variância e AGC, amplia a capacidade de identificação de descontinuidades estruturais, favorecendo interpretações sísmicas mais robustas, mesmo em áreas de elevada complexidade geológica (Chopra & Marfurt, 2007; Nanda, 2016).

3.2 – Interpretação Sísmica

A interpretação sísmica é o processo de análise dos dados de reflexão com o objetivo de construir modelos geológicos da subsuperfície. Por meio da identificação e correlação de refletores sísmicos, é possível inferir a geometria estrutural, o empilhamento estratigráfico e até as características litológicas das unidades analisadas. Esse processo depende fortemente da qualidade dos dados, da resolução vertical e lateral da imagem sísmica e do conhecimento prévio da geologia da área (Nanda, 2016).

Nos dados 2D, a interpretação geralmente se dá em perfis verticais, exigindo correlação lateral entre seções separadas, o que pode introduzir incertezas em ambientes com geometria estrutural complexa. Já nos dados 3D, a interpretação se beneficia de uma visualização volumétrica contínua da subsuperfície, permitindo cortes em múltiplas direções (inline, crossline e time-slices), o que favorece a identificação de estruturas como falhas, canais, domos e discordâncias, com maior grau de precisão (Chopra & Marfurt, 2007).

Um passo essencial na interpretação é a calibração sísmica, que consiste no ajuste espacial dos refletores sísmicos com base em dados de poço ou modelos de velocidade. Esse processo assegura que os refletores estejam posicionados em suas localizações geológicas reais, evitando distorções causadas pela geometria do meio ou por efeitos fora do plano. A calibração é ainda mais eficiente em volumes 3D, nos quais artefatos estruturais e descontinuidades podem ser corrigidos e realocados com maior fidelidade (Yilmaz, 2001).

Além da análise visual dos refletores, a interpretação moderna se apoia fortemente na aplicação de atributos sísmicos, que destacam variações sutis em amplitude, continuidade, rugosidade ou frequência. Atributos como Variância e AGC são particularmente úteis para realçar falhas, fraturas e zonas de perturbação, enquanto atributos instantâneos (frequência, fase e amplitude) auxiliam na caracterização de fácies e limites estratigráficos. A combinação de atributos em dados 3D permite extrair informações estruturais com mais clareza e delinear feições associadas à migração de fluidos (Chopra & Marfurt, 2007).

Por fim, a interpretação sísmica deve ser sempre integrada a outros dados, especialmente perfis de poço, dados geológicos regionais e modelos petrofísicos. Essa integração reduz as incertezas, aumenta a confiabilidade das interpretações e permite associar as respostas sísmicas a propriedades de reservatórios, como porosidade, litofácies e zonas de fluxo preferencial (Nanda, 2016; Yilmaz, 2001).

3.3 - Atributos Sísmicos

Atributos sísmicos correspondem a operações matemáticas aplicadas aos dados sísmicos com a finalidade de realçar propriedades específicas do sinal, permitindo a extração de informações quantitativas que, muitas vezes, não são perceptíveis em seções sísmicas convencionais. Essas ferramentas ampliam a capacidade interpretativa ao evidenciar variações sutis relacionadas a aspectos estruturais, estratigráficos ou petrofísicos dos dados, fornecendo suporte crucial para a caracterização de reservatórios e para a detecção de feições geológicas relevantes. Esses atributos podem realçar padrões estruturais, conteúdo de fluidos ou propriedades mecânicas, contribuindo para uma interpretação mais detalhada da subsuperfície. A interpretação baseada em atributos permite reduzir incertezas, revelar heterogeneidades e orientar modelos geológicos mais realistas (Chopra & Marfurt, 2007).

Os atributos podem ser classificados em diferentes categorias, conforme sua origem e finalidade. Atributos geométricos (como continuidade, variação de amplitude e rugosidade) destacam a morfologia dos refletores e são úteis na detecção de falhas, fraturas e discordâncias. Atributos instantâneos, como amplitude, fase e frequência, são derivados analiticamente do traço sísmico e fornecem subsídios para a compreensão de mudanças litológicas e variações de fácies. Já os atributos derivados de transformações estatísticas ou espectrais, como variância, energia ou similaridade, ajudam na caracterização de zonas caóticas, condutos verticais e estruturas perturbadas (Nanda, 2016).

Neste estudo, o Controle Automático de Ganho (AGC) se destaca por sua capacidade de compensar a atenuação do sinal sísmico em profundidade, por meio do balanceamento local de amplitudes. Esse procedimento preliminar contribui para a melhoria da visualização de refletores sutis ou localizados em zonas mais profundas, sem alterar a geometria original dos eventos. Embora não se constitua um recurso interpretativo direto, o AGC representa uma ferramenta essencial para o realce visual de feições geológicas em seções sísmicas com grande variação de amplitude ao longo do tempo de percurso (Yilmaz, 2001; Chopra & Marfurt, 2007).

O atributo essencial é a Variância, que mede a variação lateral dos sinais refletidos e é particularmente eficaz na delimitação de descontinuidades estruturais, como falhas e zonas de fratura. Em seções 3D, a Variância permite identificar condutos verticais de fluidos, vents ou zonas caoticamente silicificadas. O valor da variância aumenta em regiões com interrupção da continuidade sísmica, facilitando a delimitação de *geobodies* com comportamento anômalo (Chopra & Marfurt, 2007; Nanda, 2016).

A eficácia dos atributos sísmicos está diretamente relacionada à resolução dos dados e à qualidade do pré-processamento. Em ambientes complexos, a interpretação multivariada e a sobreposição de volumes atributivos permitem análises mais completas, revelando padrões estruturais e estratigráficos que podem passar despercebidos em interpretações convencionais. A integração desses atributos com dados de poço e conhecimento geológico regional é essencial para associar feições sísmicas a propriedades reais do reservatório (Yilmaz, 2001).

Capítulo 4 – Resultados

4. RESULTADOS

Artigo submetido na revista Sedimentary Geology sob o título:

Stratigraphic control over hydrothermal silicification in the Afonso Bezerra Fault, Potiguar Basin, Brazil

Abstract

Hydrothermal silicification has a significant impact on petrophysical properties of reservoir rocks. The main constraints on silica-rich fluids are the faults, their damage zones, and variations in the host lithology. However, although the influence of host lithology on silicification is partially understood, further studies are required to clarify its role and spatial impact. In this study, the Cretaceous sequences of the Potiguar Basin, comprising the sandstones of the Açu Formation and the limestones of the Jandaíra Formation, as well as the crystalline rocks of the Neoproterozoic basement, are crosscut by the Afonso Bezerra Fault System, where significant occurrences of hydrothermal silicification are observed from the basement to the surface. This study employed seismic data, along with well data, and applied seismic attributes to enhance the visualization and mapping of stratigraphic units and the geometry of the hydrothermal silicification. A statistical spatial analysis of the silicified body was conducted to assess the relationship between silicification and stratigraphy. The results revealed that silicified body concentrate along the strike of the Afonso Bezerra Fault, which appears to be the main conduit controlling the uprise of hydrothermal fluids. Width variations and shape changes of the silicified zone connected to the variations of lithology. Carbonate rocks exhibit extensive silicification associated with wider volumes of affected rocks, whereas siliciclastic rocks show narrower and less pervasive silicification. In the crystalline basement, silicification is confined to fault zones. This spatial distribution evidences the primary control of tectonics and host lithology on hydrothermal fluid flow, thereby enhancing our understanding of hydrothermal silicification compartmentalization.

Keywords: Silicification, hydrothermal vents, seismic attributes, fluid escape.

1. Introduction

Hydrothermal silicification is a post-diagenetic process that significantly modifies the petrophysical properties of host lithologies (Bjorlykke and Egeberg, 1993; Ngwenya et al., 2000; Palhano et al., 2023). From a hydrodynamic perspective, upward silica-rich fluid flows along deep-seated faults and fractures, generating high-conductivity pathways that facilitate migration while also forming low-permeability barriers, which are critical for reservoir compartmentalization (Klimchouk, 2017; Palhano et al., 2023; Rocha et al., 2025). For instance, silica precipitation alters the petrophysical properties, including porosity and permeability, of both sedimentary sequences and basement rocks in the Potiguar Basin (Menezes et al., 2019), Rio do Peixe Basin (Palhano et al., 2023; Maciel et al., 2024; Rocha et al., 2025), Thrace Basin (Berio et al., 2025a,b), Tarim Basin (Lu et al., 2017; You et al., 2018), Qiongdongnan Basin (Chen et al., 2021), and Brazilian Pre-salt Basins (Lima et al., 2019, 2020; Fernandez-Ibanez et al., 2022; Strugale et al., 2024; Corrêa et al., 2025).

The spatial distribution and shape of silicified bodies are fundamental for reservoir characterization in sedimentary basins, as they exert a direct influence on fluid connectivity and migration within the petroleum system (La Bruna et al., 2021; Corrêa et al., 2025; Rocha et al., 2025). The width of silicified bodies exhibit both lateral and vertical variability, which are controlled by local stratigraphy (Souza et al., 2021). In particular, porous layers enhance hydrothermal fluid migration, whereas impermeable layers act as barriers to the fluid flow (Souza et al., 2021; Palhano et al., 2023). Furthermore, structural heterogeneities play a decisive role in reservoir connectivity and compartmentalization. Both the structural and stratigraphic factors are critical for the development of precise and effective reservoir models (Souza et al., 2021).

Hydrothermal silicification is predominantly controlled by fault zones (La Bruna et al., 2021; Palhano et al., 2023) and by stratigraphic architecture (Souza et al., 2021). In both scenarios, the rheological behavior of the host rock plays a crucial role in determining the extent and impact of the hydrothermal process. In carbonate units, silicification can induce secondary porosity through the formation of vugs and interconnected fractures, enhancing local permeability and generating high-porosity zones that act as preferential conduits for hydrocarbon migration (Fernandez-Ibanez et al., 2022; Basso et al., 2023; Corrêa et al., 2025). Consequently, the hydrothermal process in carbonate units facilitates extensive rock dissolution, leading to a significant increase in porosity and permeability (Menezes et al., 2019; Bezerra et al., 2021). Conversely, in siliciclastic rocks, the hydrothermal process primarily promotes silica precipitation, which results in a marked reduction in porosity and permeability (Palhano et al., 2023; Berio et al., 2025a,b). This silica precipitation enhances mechanical compaction, significantly decreasing permeability and creating barriers that confine fluids, ultimately contributing to the formation of structural and stratigraphic traps (Palhano et al., 2023). Likewise, in crystalline lithologies, silica precipitation tends to be localized, primarily occurring along fault zones and fracture networks, where silica-rich hydrothermal fluids modulate hydraulic conductivity. The silicification process exhibits considerable heterogeneity across compact, impermeable zones affected by intense cementation, while permeable fractures characterized by vuggy porosity emerge as the result of multiple episodes of dynamic and static silicification (Menezes et al., 2019; Bezerra et al., 2021; Maciel et al., 2024). Although several studies have described this process, the influence of stratigraphy on the silicification process and the extent of silicification within each stratigraphic unit affected by faults remains a matter of debate.

The Potiguar Basin, located in the northeastern part of the Brazilian Equatorial Margin (Figure 1), has a complex tectonic evolution associated with rifting and oceanic spreading (drifting) processes (Matos, 1992; Pessoa Neto et al., 2007; de Castro et al., 2012; Melo et al., 2016; Lopes et al., 2018). Its structural setting, characterized by horsts, grabens, and fault systems that have undergone recurrent reactivation, exerts significant control over hydrothermal fluid circulation (Menezes et al., 2019; Bezerra et al., 2021). These processes play a decisive role in extensive silicification events along fault zones (Menezes et al., 2019; Bezerra et al., 2021), developing secondary porosity and enhancing reservoir connectivity. As a result, hydrothermal fluid migration through the overlying formations is influenced by these structural dynamics (Bezerra et al., 2009).

Advances in the analysis of hydrothermal vents have been achieved through the application of seismic techniques, including the gain equalization filter known as automatic gain control (AGC) and the variance seismic attribute, which enhance the visualization of vertical conduits and fluid escape zones while also delineating fault structures and emphasizing zones of pronounced structural heterogeneity (Maestrelli et al., 2017; Chen et al., 2021; Oliveira et al., 2023). Thus, the integrated use of the AGC filter and the variance attribute represents a fundamental approach for the precise delineation of irregular geobodies, the identification of fluid migration pathways, and the characterization of width variations in formations affected by silicification and fracturing. This methodology significantly enhances the accuracy of seismic reservoir characterization, providing deeper insights into the subsurface architecture of the hydrothermal bodies.

This study investigates the relationship between the width of a silicified geobody and the lithology of the host units within the Potiguar Basin, located in northeastern Brazil (Fig. 1). We set this goal to fill some gaps, such as: (i) How do the different lithologies (crystalline, siliciclastic, and carbonate units) affect the width of silicified body? (ii) Does the transition between these units influence the width of silicified body? (iii) What is the effect of faults on the width of silicification? (iv) Do hydrothermal vents exhibit internal heterogeneities, in which portions of the host rock remain unaffected by silicification or are only partially overprinted, suggesting that silicification is selective and does not fully pervade the entire conduit geometry? To answer these questions, seismic data, processed with AGC and Variance attribute, were utilized to delineate silicified zones and their lithological controls. Additionally, we examined the structural influence of the Afonso Bezerra Fault System (ABFS) on the spatial distribution and shape variability of the silicified geobody. The findings provide critical insights into the impact of hydrothermal silicification on reservoir properties across diverse lithologies, offering a robust framework for refining exploration models and enhancing predictions of reservoir quality in structurally complex settings.

2. Geological Setting

The Potiguar Basin occurs within the eastern segment of the Brazilian Equatorial Margin and covers approximately 60,000 km² (Fig. 1). The Potiguar Basin comprises both onshore and offshore domains, structurally marked by horsts and grabens that developed through three distinct phases – rift, post-rift, and drift – since the Cretaceous (Bertani et al., 1990; Pessoa Neto et al., 2007). The basin's formation and development are closely linked to the opening of the South Atlantic Ocean and the fragmentation of Pangea (de Castro et al., 2012), underscoring the basin's significance in regional geodynamic evolution.

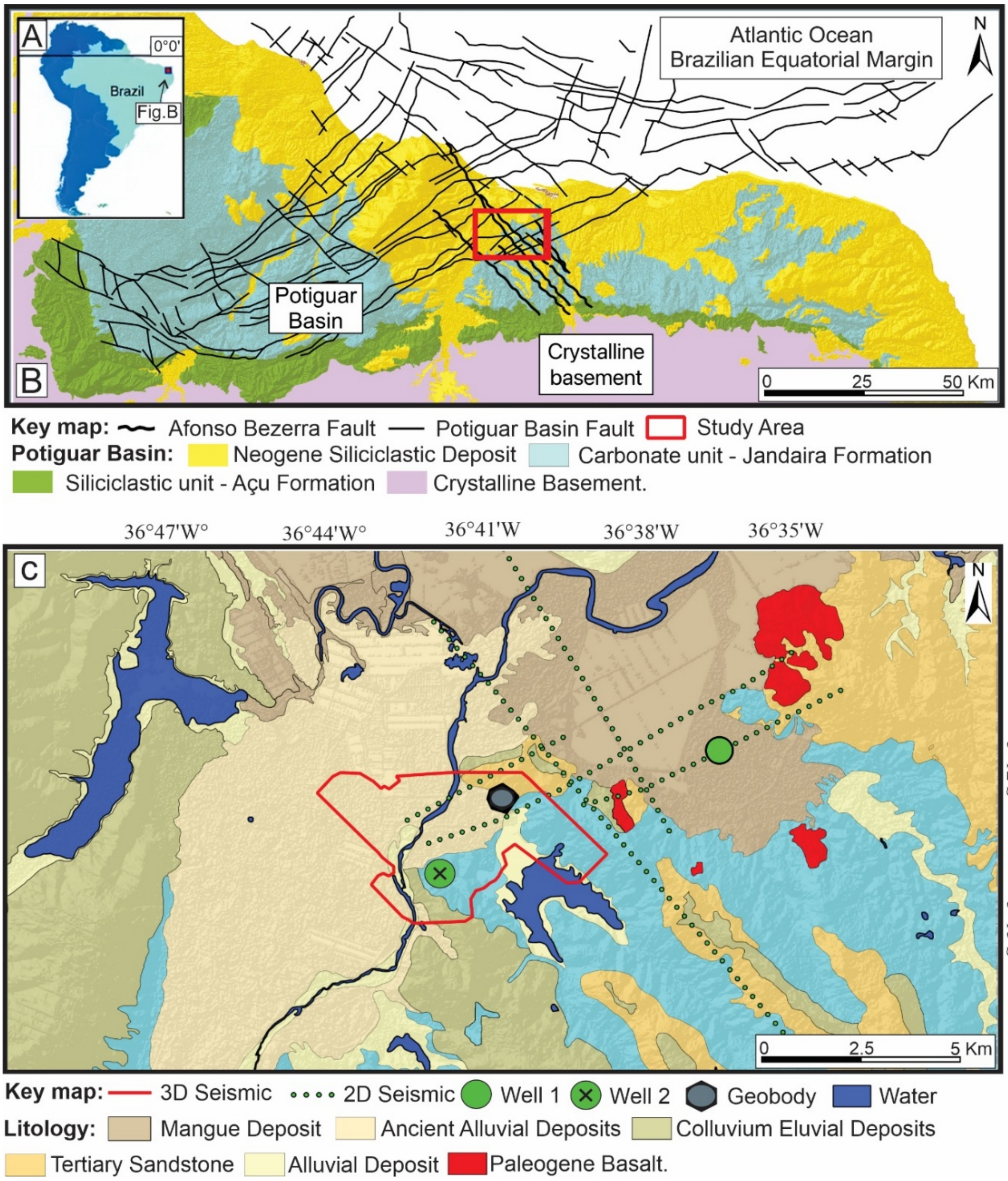

Figure 1. (A) The South American Continent and the location of the Potiguar Basin. (B) Location map of the Potiguar Basin in northeastern Brazil. Modified from Bertani et al. (1990), Bezerra et al. (2009), and de Castro and Bezerra (2015). The Afonso Bezerra Fault System is marked in bold and the study area. (C) Geological-structural map of the study area showing the dataset, including a 3D seismic cube, 2D seismic lines, geobody, and wells used for

lithostratigraphic correlation The features used in this map are based on Bezerra et al. (2009).

The rift phase of the Potiguar Basin was initiated in the Neocomian, driven by significant crustal extension that led to the formation of half-graben systems controlled by normal faults and pre-existing discontinuities (Matos, 1992; de Castro et al., 2012). These structural compartments provided accommodation space for fluvial and lacustrine sediment accumulation, forming the Rift Supersequence (Fig. 2). The stratigraphic record of this phase includes the Pendência Formation, composed of conglomeratic sandstones and lacustrine shales, and the Pescada Formation, consisting of coarse sandstones and pelitic intervals – both preserve evidence of extensive alluvial fan and fluvio-deltaic systems under prevailing tectonic influence (Araripe and Feijó, 1994; Pessoa Neto et al., 2007).

The end of rifting activity in the Aptian marked the onset of the post-rift phase, predominantly controlled by thermal subsidence and a gradual shift from continental to shallow marine depositional environments (Pessoa Neto et al., 2007). This phase represents a period of relative tectonic quiescence, characterized by widespread marine transgression, resulting in the deposition of the Alagamar Formation. This unit, composed of fine sandstones, shales, and micritic limestones, is interpreted as a transitional depositional system that records the evolving paleoenvironmental conditions associated with post-rift basin dynamics (Pessoa Neto et al., 2007; Melo et al., 2020).

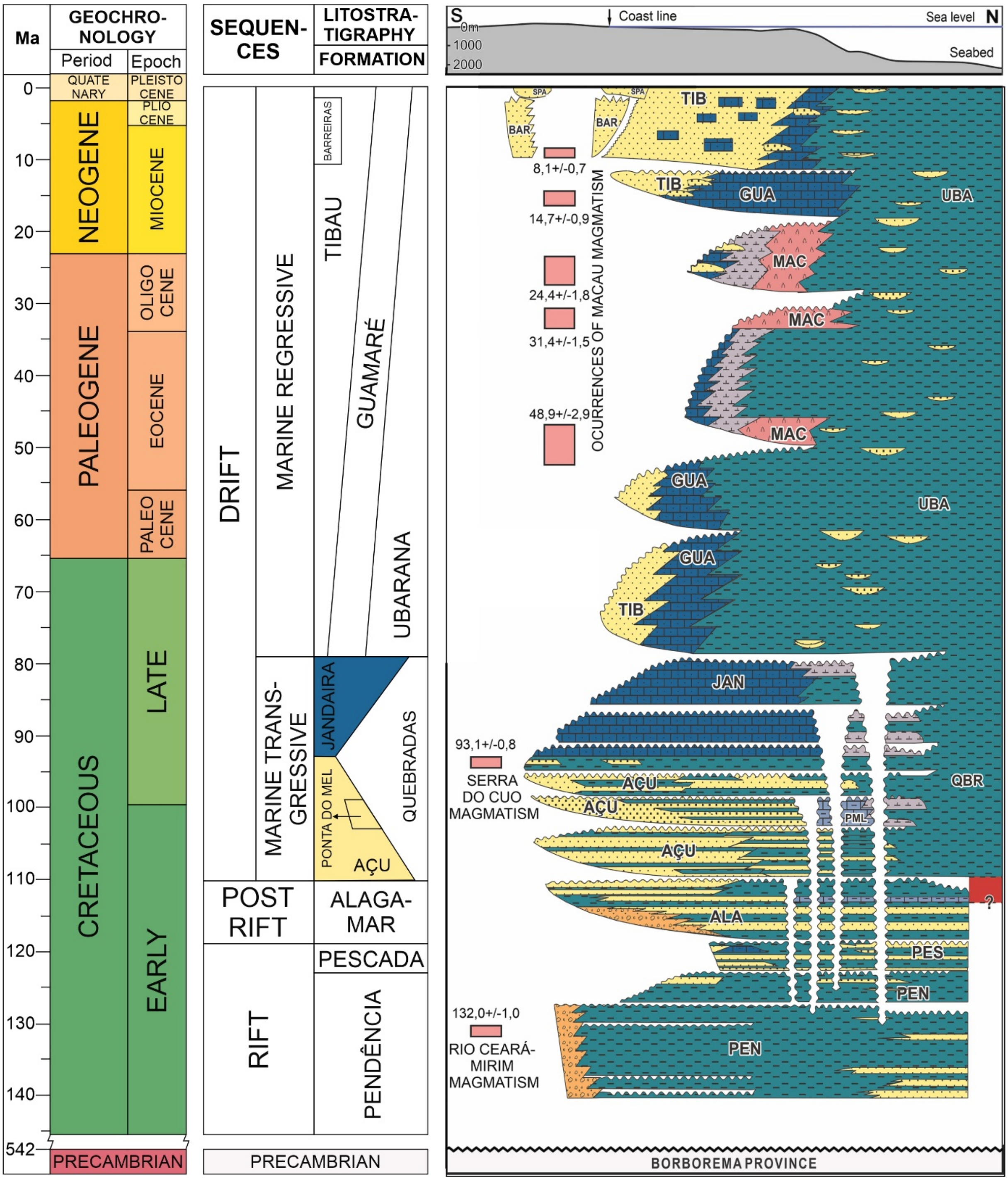

Figure 2. Simplified stratigraphic column of the Potiguar Basin, showing the main formations from the rift, post-rift, and drift phases, as well as the underlying crystalline basement units. The Alagamar, Açu, and Jandaíra formations represent the key units analyzed in this study. Modified from Pessoa Neto et al. (2007) and Cunha et al. (2021).

Initiated in the Albian within a passive margin framework, the drift phase was characterized by extensive marine sedimentation modulated by second- and third-order transgressive-regressive cycles that marked the interfingering of continental and marine depositional systems (Melo et al., 2020). The Açu Formation, composed of coarse to medium-grained fluvial sandstones with interbedded pelitic layers, indicates fluvial deposition under high-energy conditions. The Ponta do Mel Formation, comprising oolitic calcarenites and shales, documents sedimentation within a shallow carbonate continental shelf influenced by tides. The Quebradas Formation, dominated by marine shales and turbidites, reflects deposition in continental slope and deep-marine basin settings. Overlying these units, the Jandaíra Formation – bioclastic limestones and dolomites – records the establishment and development of an extensive carbonate ramp from the Turonian to the Campanian (Cremonini, 1993; Pessoa Neto et al., 2007). However, only the Açu and Jandaíra Formations are located in the study area.

The basement underlying the Potiguar Basin has Precambrian age and is associated with the Borborema Province. It originated from the amalgamation of Archean and Paleoproterozoic crustal blocks (Almeida et al., 1981) and comprises a complex assemblage of igneous and metamorphic rocks, including gneisses, schists, migmatites, and quartzites, linked to the Caicó Complex and the Seridó Group (Almeida et al., 1981). This basement exerts a fundamental control over the basin's structural framework, influencing sedimentary deposition patterns and the development of the petroleum system (de Castro et al., 2012).

The structural framework of the onshore Potiguar Basin is primarily controlled by NE–SW-trending fault systems formed during the Early Cretaceous rifting phase. These structures define graben and horst systems associated with regional crustal thinning, resulting from lithospheric rupture between the Borborema Province (Brazil) and the Benin Province (Nigeria) during the opening of the South Atlantic Ocean (Matos, 1992; de Castro et al., 2012). Brittle reactivation of ductile shear zones within the crystalline basement, particularly the Portalegre Shear Zone, facilitated the nucleation of high-displacement normal faults, including the Carnaubais Fault, the principal fault of the Potiguar rift system (de Castro et al., 2012; Melo et al., 2016; Menezes et al., 2019).

In addition to the dominant NE–SW fault system, the onshore part of the Potiguar Basin is also transected by NW–SE-oriented structures, most prominently the Afonso Bezerra Fault System (ABFS, Fig. 1B), a network of subparallel faults extending up to 90 km (Bezerra et al., 2006; Menezes et al., 2019). The ABFS remained active from the rifting through the post-rift stages, exerting significant control over the depositional and post-depositional processes affecting siliciclastic and carbonate successions, particularly the Açu and Jandaíra formations (Moura-Lima et al., 2011; Menezes et al., 2019). Post-rift fault reactivation under dynamic stress regimes induced strike-slip and transpressional movements, triggering hydrothermal fluid migration and pervasive silicification along fault-controlled zones (Bezerra et al., 2006; Menezes et al., 2019). Additionally, a subsequent basin inversion event further reshaped the basin’s morpho-structural framework (Bezerra et al., 2020, 2023).

The Potiguar Basin exhibits extensive hydrothermal silicification along fault zones, particularly in the ABFS, where tectonic reactivation has facilitated the migration of silica-rich fluids and their interactions with variable lithologies, influencing rock properties (Bezerra et al., 2006; Moura-Lima et al., 2011; Menezes et al., 2019). This fault network acts as a preferential conduit for silica-rich hydrothermal fluids, significantly affecting the crystalline basement, siliciclastic, and carbonate successions (Menezes et al., 2019). Field and petrophysical investigations reveal multiple episodes of fluid migration, resulting in intense mineralogical replacement and large-scale alteration of the original rock framework (Menezes et al., 2019). Variation in widths of silicified zones suggests a strong stratigraphic influence on fluid distribution, directly impacting the petrophysical properties, fluid compartmentalization, and hydrocarbon reservoir potential through secondary porosity generation (Bezerra et al., 2006; Menezes et al., 2019).

3. Data and Methods

Seismic and well data utilized in this study were obtained from the Brazilian Agency for Petroleum, Natural Gas, and Biofuels (ANP) to support the geological-geophysical assessment of the research area. These datasets are freely available through a collaborative agreement between ANP and the Geological Survey of Brazil (SGB), all accessible via the REATE Project online platform. An industry-standard approach, using the Petrel® software platform by Schlumberger Information Solutions, was employed for data interpretation, enabling the delineation of stratigraphic framework, thereby ensuring a comprehensive evaluation of subsurface conditions.

3.1. 2D and 3D Seismic Data

The seismic dataset comprises 2D and 3D seismic data, designed to provide regional coverage and a robust basis for geophysical analysis (Fig. 1C). The dataset adheres to the SEG convention, featuring inverted polarity, and was preprocessed, migrated, and provided in two-way travel time (TWT) (milliseconds) with spatial dimensions in meters. Two 2D seismic lines were employed to integrate lithostratigraphic information into the 3D seismic cube (Fig. 1C).

The 3D seismic volume consists of 429 inlines and 594 crosslines, oriented NW-SE and NE-SW, respectively, with a spatial resolution of 15 m per inline and crossline. The total extent of the seismic cube is approximately 8,896 m in the inline direction and 6,420 m in the crossline direction, encompassing a significant portion of the study area. Two wells were incorporated to achieve two primary objectives: (1) to use check-shot data for seismic-well tie calibration and depth correlation, and (2) to validate the lithological controls of the selected geobody, interpreted as hydrothermal vent-related. Well data were essential for surface mapping and seismic stratigraphic interpretation, providing crucial constraints for geological modeling.

The workflow developed for this study followed five main steps: (1) seismic-well tie and depth calibration; (2) mapping of stratigraphic interfaces and surface modeling; (3) seismic stratigraphic interpretation; (4) application of seismic techniques, including the use of the gain equalization filter (AGC) and the variance seismic attribute analysis; and (5) mapping and analysis of the geobody of the hydrothermal silicification.

In the preliminary mapping of the 2D and 3D seismic data, several potential vents were identified based on their characteristic seismic signatures. Subsequently, a single vent was selected for a more in-depth analysis, using interpretative criteria grounded in the use of AGC (Automatic Gain Control) and Variance, as this vent exhibited the most prominent contrasts, making it the most suitable for data extraction and three-dimensional modeling in the context of this study.

3.2. Seismic Interpretation

Seismic reflection data interpretation in this study involved identifying and correlating subsurface stratigraphic units through the analysis of reflectivity, continuity, amplitude, and frequency of seismic reflectors, as well as correlating seismic profiles with well data. Additionally, seismic facies distribution has been interpreted as a key aspect of hydrocarbon exploration in basins with high structural and depositional complexity (Mitchum et al., 1977; Posamentier and Kolla, 2003; Catuneanu et al., 2011; Catuneanu, 2017, 2019a,b).

To map the stratigraphic surfaces, a 3D model was constructed correlating the upper boundaries of stratigraphic units with corresponding seismic horizons, utilizing stratigraphic data from wells to support seismic interpretation. From the base to the surface of the basin, the following formation tops were mapped: (1) Basement unit, (2) Alagamar Formation, (3) Açu Formation, and (4) Jandaíra Formation. However, the Jandaíra Formation outcrops at the present-day topographic surface, preventing the seismic interpretation of its uppermost section. The quality of seismic data was critical for the accuracy of horizon delineation, as reflector resolution and continuity were essential for identifying the formation boundaries. Data limitations resulted in the identification of noisy areas from 0 to 200 ms (TWT) and below the Basement unit, which impacted the definition of horizons and the characterization of geological features.

3.3. Seismic Attributes

In this study, AGC and Variance attributes were applied to improve the identification of hydrothermal vents and delimit the seismic horizons affected by fluid migration. AGC is a fundamental seismic processing technique that automatically adjusts signal amplitudes along seismic profiles (Yilmaz, 2001; Chopra and Marfurt, 2007). This attribute improves the continuity, resolution, and clarity of weak reflectors, particularly in stratigraphically complex or geologically noisy environments (Maestrelli et al., 2017; Chen et al., 2021; Oliveira et al., 2023).

In the study area, this attribute compensated for the attenuation of seismic energy with depth, ensuring the visibility of deep reflectors, which highlighted the continuity of the low-amplitude reflectors from the Açu Formation. Additionally, AGC enhances amplitude uniformity, which facilitates the identification of stratigraphic boundaries and geological structures, and optimizes the signal-to-noise ratio, allowing for more accurate interpretation of the stratigraphic limits (Li et al., 2024; Pang et al., 2024). This technique is particularly effective in environments characterized by high-amplitude variability and is commonly applied to both land and marine seismic datasets (Kahrizi et al., 2014; Li et al., 2022; Karmanov et al., 2024; Nasıf, 2024; Araque-Pérez et al., 2024). In this study, we utilized the AGC to enhance and highlight the low-amplitude horizons.

The Variance attribute is crucial for seismic data analysis of geological discontinuities, such as faults and fractures, which may be overlooked in conventional interpretation methods (Marfurt et al., 1998; Chopra and Marfurt, 2007). As a coherence-based attribute, it was applied to highlight fluctuations in seismic amplitudes within a specific window, thereby enhancing the detection of abrupt changes in the subsurface and refining the identification of features associated with hydrothermal vents, fault-related discontinuities, fluid escape structures, and other geologically complex systems. This approach ensured a more accurate representation of fluid pathways within the study area, specially identifying lateral discontinuities and zones of high structural heterogeneity, such as small faults associated with the ABFS. Previous studies have demonstrated the effectiveness of Variance in interpreting seismic features associated with hydrothermal fluid migration and identification of gas escape structures (Davies, 2003; Huuse and Mickelson, 2004; Berndt, 2005; Chopra and Marfurt, 2005; Huuse et al., 2010; Hustoft et al., 2010; Moss and Cartwright, 2010; Løseth et al., 2011; Cartwright and Santamarina, 2015; Maestrelli et al., 2017; Oliveira et al., 2023; Ismail et al., 2024).

3.4. Statistical Analysis of the Silicification Width

A statistical analysis was conducted to evaluate the dispersion halos of silicified zones across the basin stratigraphy. The methodology examined patterns of heterogeneity and concentration within the silicified zones, refining previous approaches applied by Maestrelli et al. (2017) in a distinct geological context, where the hydrothermal vent corresponds to silicified rocks, as shown by Menezes et al. (2019). In this study, an integrated interpretation and geophysical analysis were incorporated to enhance the understanding of the lithological controls on silicification.

Seismic data were analyzed in both the crosslines and inline directions, with measurements taken at intervals of five seismic lines. A total of 10 crosslines and seven inlines were selected, resulting in 70 measurement points used to calculate the width of the hydrothermal silicification fluid pipes along the seismic sections. In this study, descriptive statistical methods were employed to compute measures of central tendency (mean and median) and dispersion (standard deviation and variance), thereby quantifying variations in silicification intensity across the stratigraphic column.

4. Results

4.1. Description of the stratigraphic Units

This section presents an interpretation of the main stratigraphic units in the study area, based on the integration of 2D and 3D seismic data with lithological information from two calibration wells (Well 1 and Well 2). The description is organized into two parts: (i) the mapping of seismic surfaces that define the top of each stratigraphic unit; and (ii) the internal configuration of the stratigraphic units, described through the analysis of seismic facies, which is based on variations in amplitude, frequency, and continuity of reflectors.

The seismic interpretation was based on the seismic-well tie (Wells 1 and 2) (Figs. 3 and 4). The first well indicates that the basement is observed at a depth of more than -531.26 ms, composed of crystalline rocks. Filling the basin, the Alagamar Formation appears from a depth of -474.00 ms, composed of conglomerate and mudstone. Additionally, the Açu Formation is found, with its limits between -181.46 ms and -474.00 ms, characterized by coarse sandstones interbedded with mudstones. At the top of this sequence, the Jandaíra Formation occurs from -181.46 ms to the surface and is composed of calcarenite. These lithological variations, as observed in the well data, are more clearly evident in the changes in seismic facies with depth (Fig. 3).

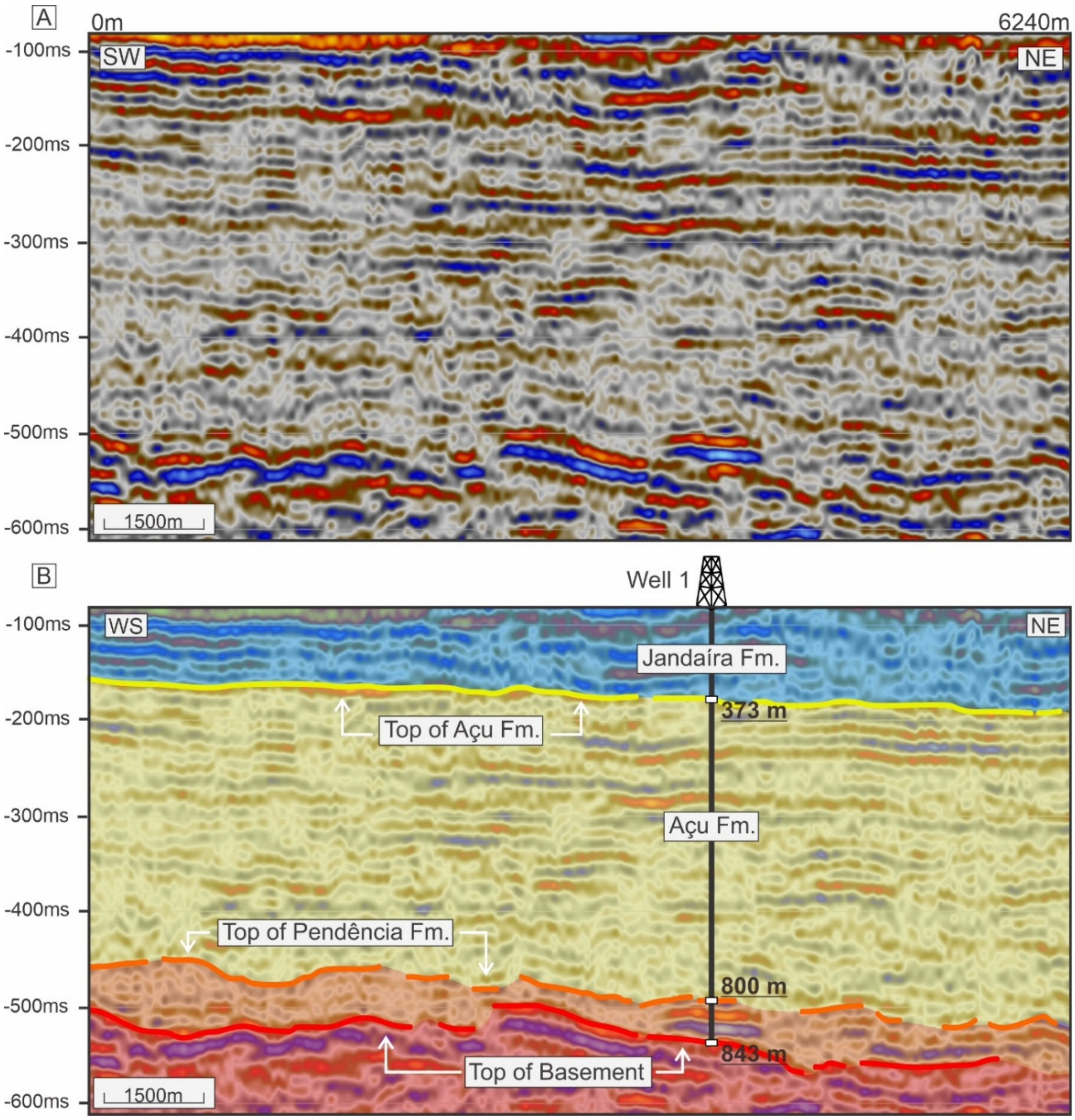

Figure 3. (A) Uninterpreted and (B) interpreted 2D seismic section with lithostratigraphic correlation based on Well 1, identifying four main units: Basement, Pendência Formation, Açu Formation, and Jandaíra Formation. See Fig. 1C for the location of this section. Vertical exaggeration: 5x.

Well 2 identified the crystalline basement at a depth approximately -806.09ms, overlain by the Alagamar Formation (-541.05ms), composed of shale, marl, and limestone. The

Açu Formation (-315.22ms) includes sandstone interbedded with shale and carbonate. The Jandaíra Formation (from -315.22ms to the surface) consists of bioclastic limestone and calcarenite (Fig. 4).

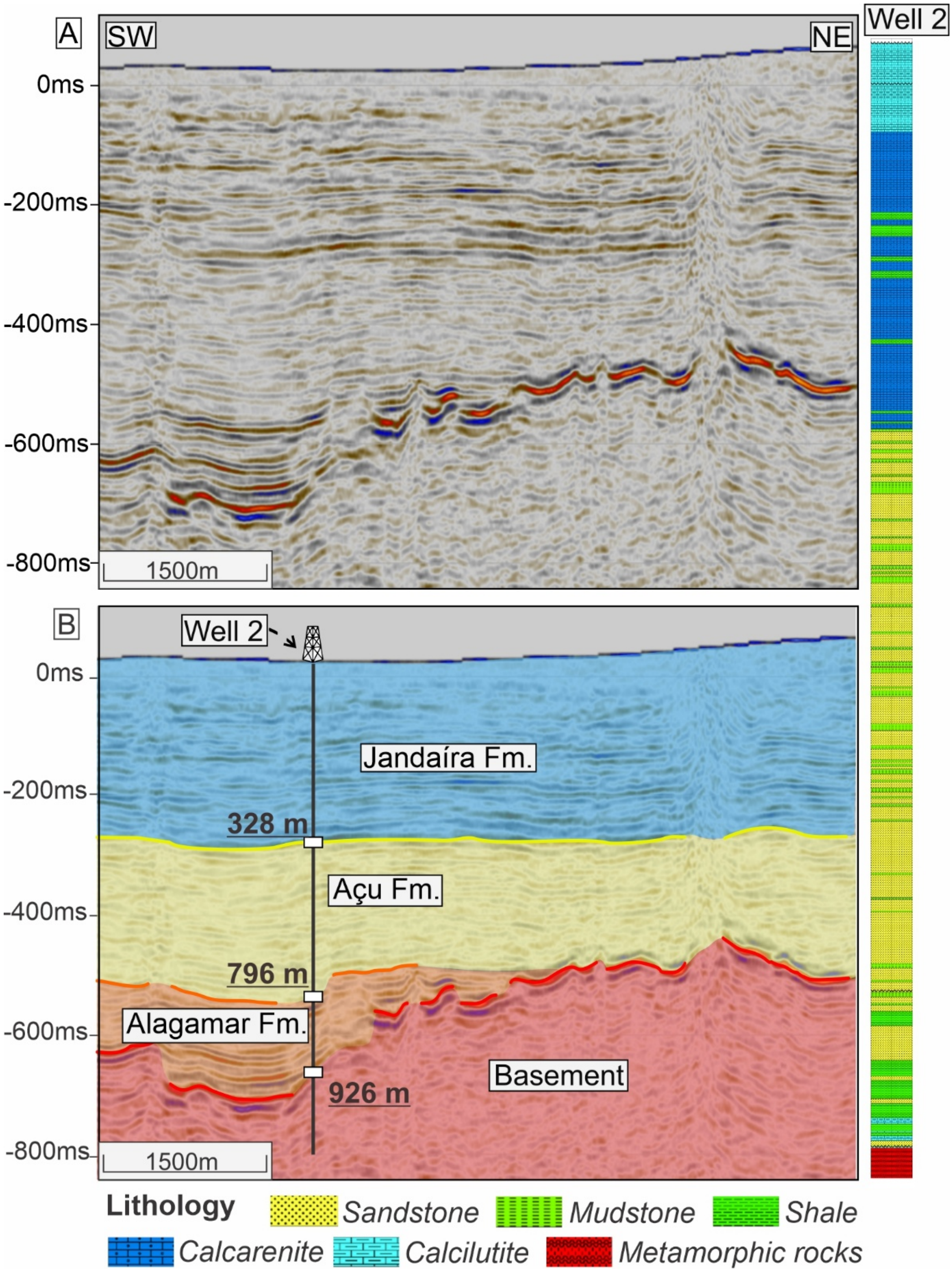

Figure 4. (A) Uninterpreted and (B) interpreted seismic section from the seismic volume with stratigraphic correlation based on Well 2, identifying four main units: Basement, Alagamar Formation, Açu Formation, and Jandaíra Formation. Unit boundaries are defined by distinct reflectors, with seismic facies variations observed as depth increases. See Fig. 1C for the location of this section. Vertical exaggeration: 5x.

The seismic data enabled the identification of four units, separated by three horizons based on different internal seismic reflector patterns (Fig. 5). The basement seismic facies (Fig. 5), composed of crystalline rocks, is marked by low-amplitude, but a high-amplitude reflector, with a chaotic internal pattern and lateral discontinuities characterize the top of this unit. Above this lies the top of the Alagamar Formation, whose seismic facies (Fig. 5) are defined by a high-amplitude, low to moderate frequency, reflectors parallel and continuous, and associated with siliciclastic rocks, such as conglomerates and mudstones (Fig. 4). The Açu Formation seismic facies (Fig. 5) feature a moderate- to low-amplitude, moderate to low frequency, reflectors parallel to subparallel, and discontinuous, associated with siliciclastic rocks, such as sandstones interbedded with mudstones (Fig. 4). At the top of the sequence, the seismic facies of the Jandaíra Formation (Fig. 5) is marked by a moderate- to high-amplitude, moderate frequency, reflectors parallel to subparallel, and continuous with some local interruptions, whose reflectors are associated with carbonate rocks (Fig. 4).

Stratigraphic units	Seismic facies	Amplitude	Frequency	Internal configuration	Continuity
Jandaíra Fm.	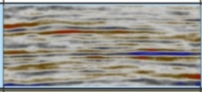	Moderate to high	Moderate	Parallel and subparallel	Continous with local interruptions
Açu Fm.	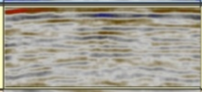	Moderate to low	Moderate to low	Parallel to subparallel	Continuous
Alagamar Fm.		High	Low to moderate	Parallel	Continuous
Basement	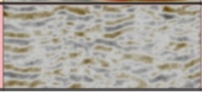	Low	Low	Chaotic and discontinuous	Discontinuous

Figure 5. Stratigraphic interpretation based on seismic reflector patterns, identifying the top of the crystalline basement, the Alagamar Formation, the Açu Formation, and the Jandaíra Formation, based on the seismic volume data.

4.2. Seismic Surfaces

We interpreted the horizons of the top of the basement, as well as the Açu and Alagamar formations, in the time domain . The upper horizon corresponding to the top of the Açu Formation presents depth variations ranging from -325 ms to -230 ms (Fig. 6A). The top surface of the Açu Formation exhibits minimal depth variation. A nearly flat geometry characterizes it, indicating a relatively uniform seismic horizon, with little structural relief or significant topographic irregularities across the mapped area (Fig. 6A).

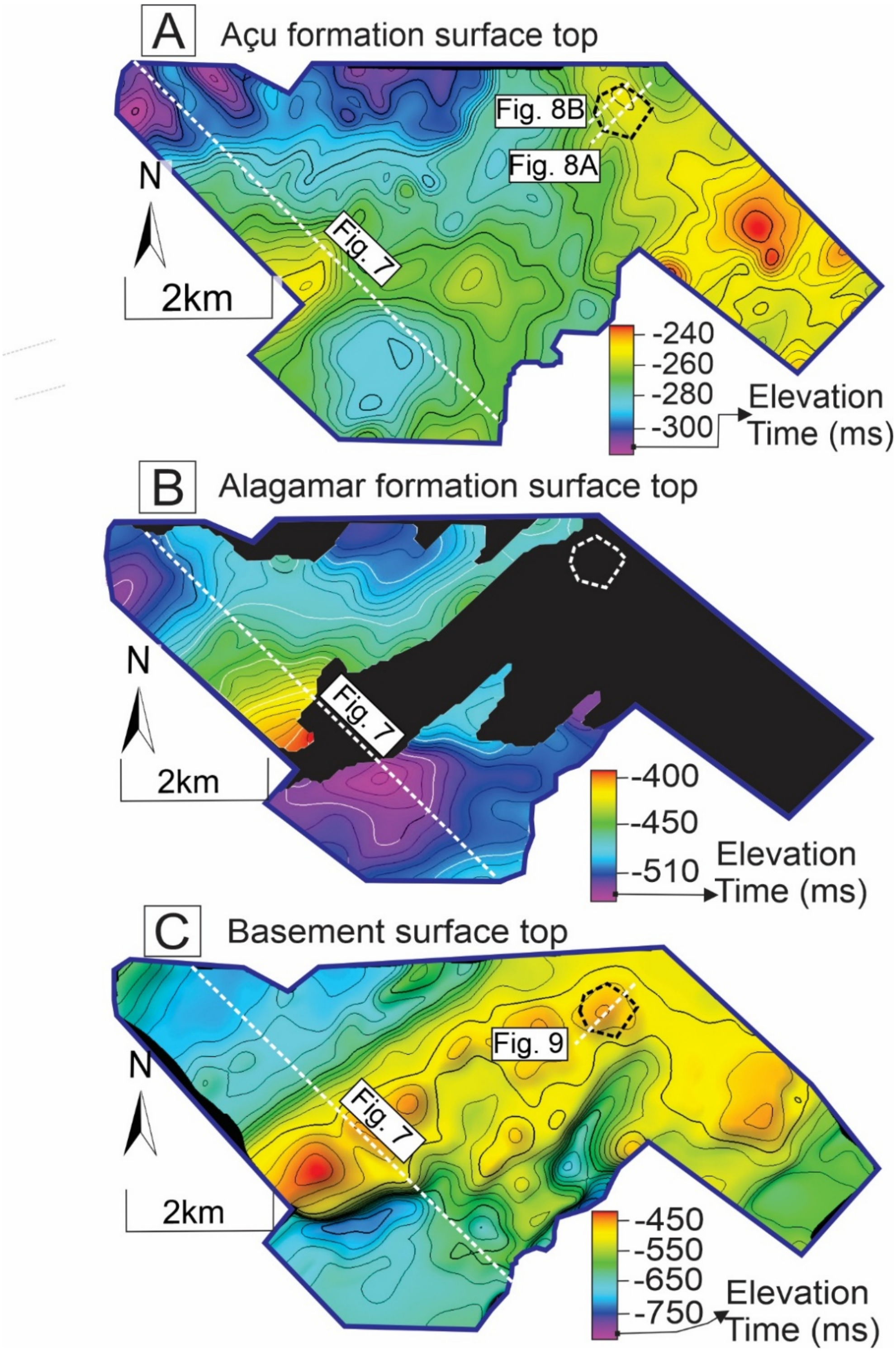

Figure 6. Seismic surfaces in TWT. (A) Açu Formation top. (B) Alagamar Formation top. (C) Basement top. The black dashed lines in A and C, and the white dashed line in C are related to the location of the hydrothermal silicification vent. Vertical exaggeration: 5x.

The seismic surface of the Alagamar Formation (Fig. 6B) indicates variations ranging from -540 ms (in purple) to -400 ms (in orange). The surface exhibits low-elevation areas (in purple and blue) predominantly distributed in the southeastern and central-western portions, which may represent grabens. The elevated zones (in orange to green), located in the central and northern parts of the area, indicate horsts. The lateral depth variation suggests the presence of tectonic control features, with an extensive faulting pattern influencing the deposition and thickness of sedimentary units.

The surface of the basement (Fig. 6C) displays depth variations ranging from -720 ms (in light blue) to -480 ms (in yellow). A highly irregular topography is observed, with structural highs (indicated in yellow and green) and lows (in blue and purple), highlighting the presence of horsts and grabens that shape the basement's architecture. This surface map highlights areas of higher elevation in the central and northeastern parts, representing horsts surrounded by NE-SW-striking faults (Fig. 6C). These elevations are associated with fault features that control the geometry of the deposits. The depressions are located in the western portion, suggesting areas of greater sedimentary thickness related to grabens or incised valleys filled during sedimentation.

Figure 7 presents an interpreted seismic section in which the main stratigraphic units of the area are highlighted: basement, Alagamar, Açu, and Jandaíra formations. The figure reveals variations in reflector continuity, amplitude, and internal geometry, allowing a clear visualization of stratigraphic contacts and the vertical organization of the formations.

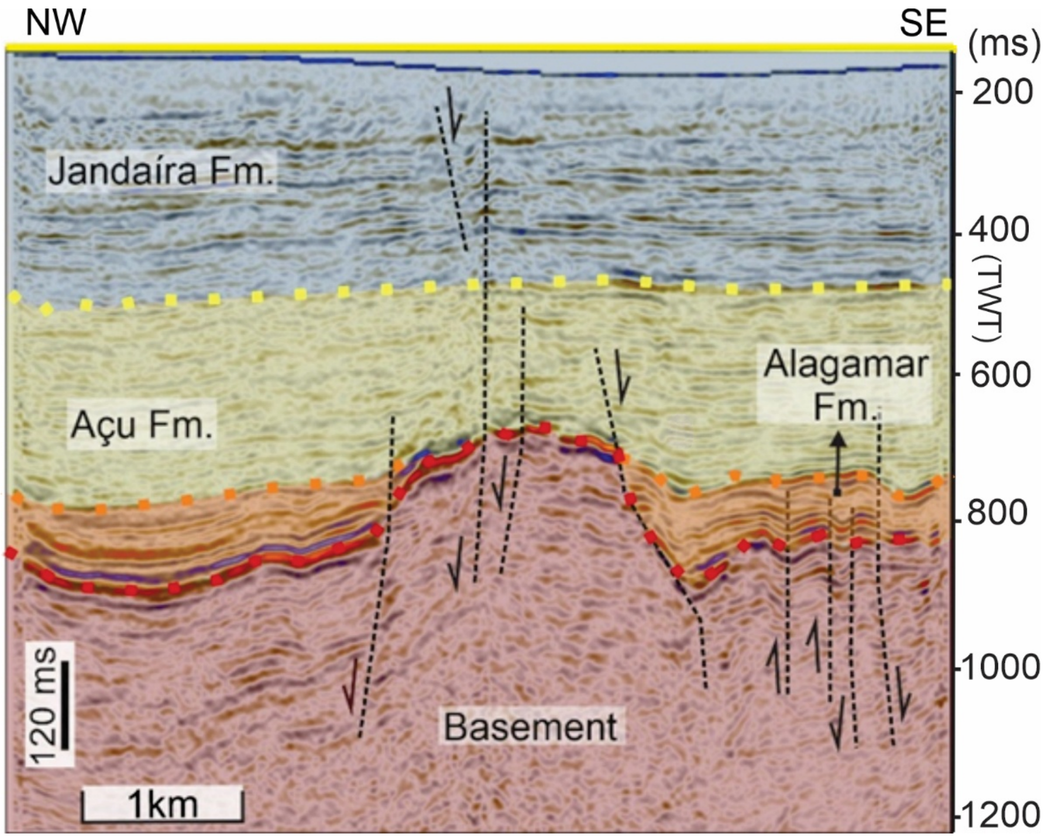

Figure 7. Interpreted seismic section showing the crystalline basement and the overlying Alagamar, Açu, and Jandaíra formations. The image highlights variations in seismic facies, reflector continuity, and stratigraphic boundaries throughout the section. The seismic sections are located in Figure 6(A,B and C). Vertical exaggeration: 5×.

4.3. Hydrothermal vent description and its geometric characterization

A hydrothermal silicification vent selected for this study, previously identified in outcrop by Menezes et al. (2019), was delineated in the seismic data through distinctive patterns of reflector scattering and amplitude attenuation. These anomalies suggest localized disruptions in acoustic continuity consistent with intense silica alteration in the subsurface, corroborating surface observations. In both inline and crossline seismic data, these structures are identifiable due to the lateral contrast in reflectors, where disturbed zones (DZs) with significant discontinuity contrast are sharply distinguished from the surrounding horizontal reflectors. Near the surface (approximately 0-200 ms), noisy zones heavily interfere with fluid pipe patterns, appearing as scattered signals and complicating interpretation in this interval. The root zone marks the fluid source unit located below the basement top, revealing the origin of the fluid and its migration pathway through the basement. The root zones of the pipes interconnect beneath the basement top, where fluids escape through individual normal faults. With this, the vents are linked to faults that connect directly to the fluid source. The "downward tapering cone" vent geometry is toward the top, cutting across all basin formations until it reaches the surface.

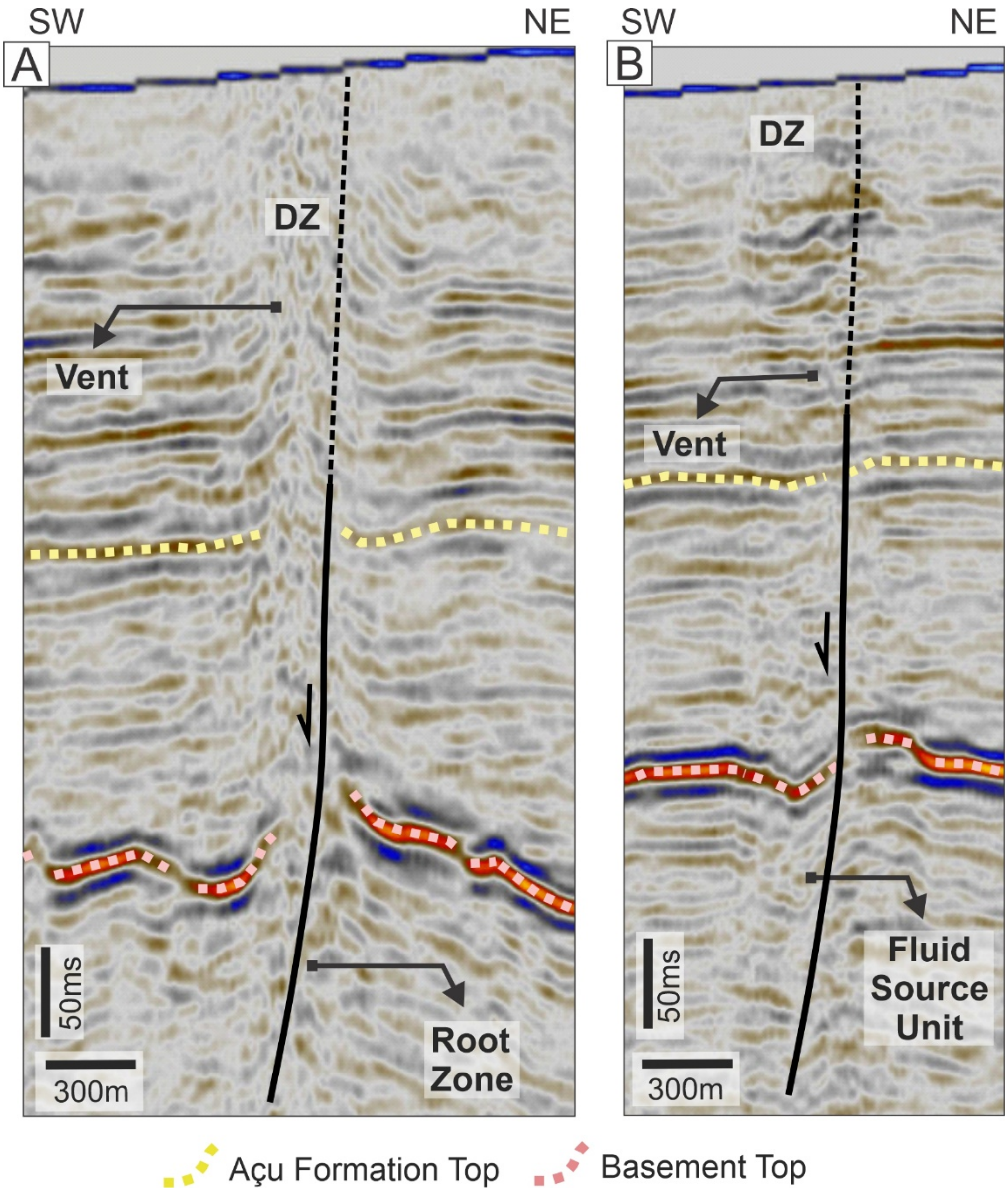

Figure 8. Seismic sections illustrate the geometry of hydrothermal vents. (A) Vents marked by disturbed zones (DZ) with disrupted reflectors and amplitude attenuation. The root zone lies below the top of the basement. (B) Vents connected to the fluid source unit by normal faults, showing the upward pathway of hydrothermal fluids through the basin formations. Vertical exaggeration: 5x. The seismic sections correspond to the geobody depicted in Figure 1C and are located in Figure 6A.

The hydrothermal vent was identified and delineated based on subsurface structural discontinuities observed in the interpreted seismic section with AGC (Fig. 9A). The application of the variance attribute further highlights the geometry of the vent and its interaction with the surrounding sedimentary formations, particularly by outlining the zone of disruption. This disturbed area is characterized by a concentration of discontinuous reflectors, which correspond to elevated positive values of the variance attribute, delineating the internal architecture and lateral boundaries of the vent (Fig. 9B).

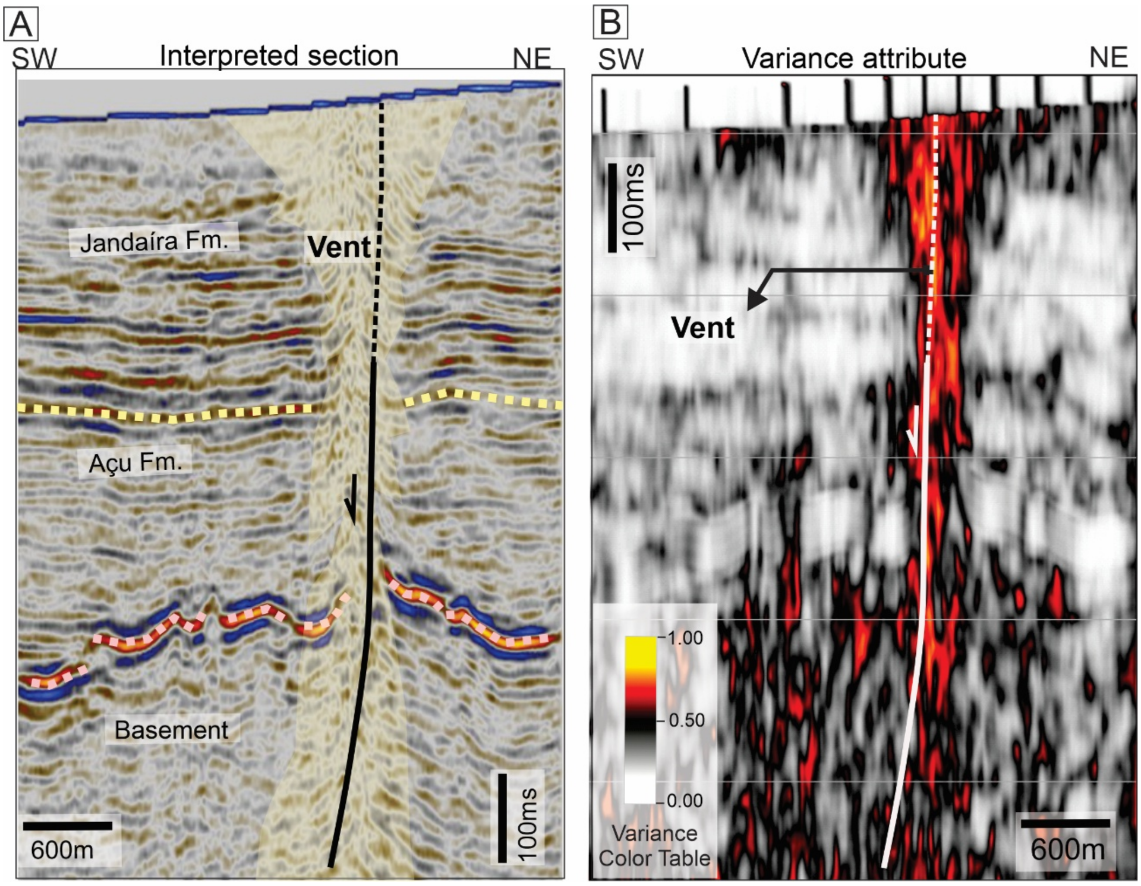

Figure 9. *(A)* Interpreted seismic section with Automatic Gain Control (AGC) applied, showing hydrothermal vent cutting through the Basement, Açu Formation, and Jandaíra Formation. *(B)* Variance attribute applied to the same section, highlighting structural discontinuities associated with the vent, revealing the internal geometry and lateral boundaries of the disturbed zone.

Vertical exaggeration: 5x. The seismic section correspond to the geobody depicted in Figure 1C and is located in Figure 6C.

Using the measured width values, central tendency metrics such as mean and median were calculated to identify the average width of the silicified body (Tab. 1 and Fig. 10). Additionally, standard deviation and variance were calculated, providing a measure of data dispersion and indicating variability in width along different crosslines and inlines. These statistical data are fundamental for determining the uniformity or heterogeneity of the selected geobody.

The statistical results, presented in Table 1, reveal a clear variation in the width of the silicified geobody across different seismic directions. In crosslines, the average width reaches 524.02 m, with a median of 505.91 m, a maximum of 869.90 m, and a higher standard deviation (27.96 m), indicating greater lateral heterogeneity in this direction. In contrast, inlines exhibit a slightly higher mean width (574.57 m) and median (611.12 m), but with lower variability (standard deviation of 13.48 m), suggesting a more continuous distribution along the fault-parallel direction. These results emphasize that the geometry of the silicified body is not uniform and is strongly influenced by the structural orientation of the ABFS, which promotes preferential pathways for fluid migration and controls the vertical and lateral extent of hydrothermal alteration.

Table 1. Statistical summary of depth (TWT) and width (m) for the analyzed silicified geobody (time-depth calibrations were based on well-to-seismic ties using checkshot data). The data is presented separately for crosslines and inlines, showing key measures of central tendency (median and mean), variability (standard deviation), and range (maximum and minimum) for

the seismic attributes. This analysis highlights the spatial variability and provides insights into the distribution of silicification in the study area.

Statistic	Depth TWT (ms) - Crossline	Width (m) - Crossline	Depth TWT (ms) - Inline	Width (m) - Inline
Mean	279.98	524.02	281.78	574.57
Median	266.87	505.91	280.77	611.12
Standard Deviation	20.34	27.96	21.16	13.48
Maximum	606.17	869.90	621.53	841.30
Minimum	50.76	187.19	50.06	185.34

The spatial distribution and geometric characterization of the silicified geobody is illustrated in Fig. 10. In the Panel A (Fig. 10A), the seismic sections highlight the main measurement points used to quantify width at six different depths, with the application of the variance attribute enhancing the visibility of disrupted zones and fault-controlled geometries. These vertical sections reveal that the propagation of silicified vents is guided by fault systems acting as conduits for hydrothermal fluids, especially along the ABFS. Panel B (Fig. 10B) displays a point cloud diagram, in which the lateral width of the silicified geobody correlates strongly with fault orientation and stratigraphic boundaries. The concentration of wider segments along specific directions indicates zones of enhanced hydraulic connectivity and focused silica precipitation. This pattern supports the interpretation that both structural and stratigraphic factors control the geometry and continuity of hydrothermal features in the study area.

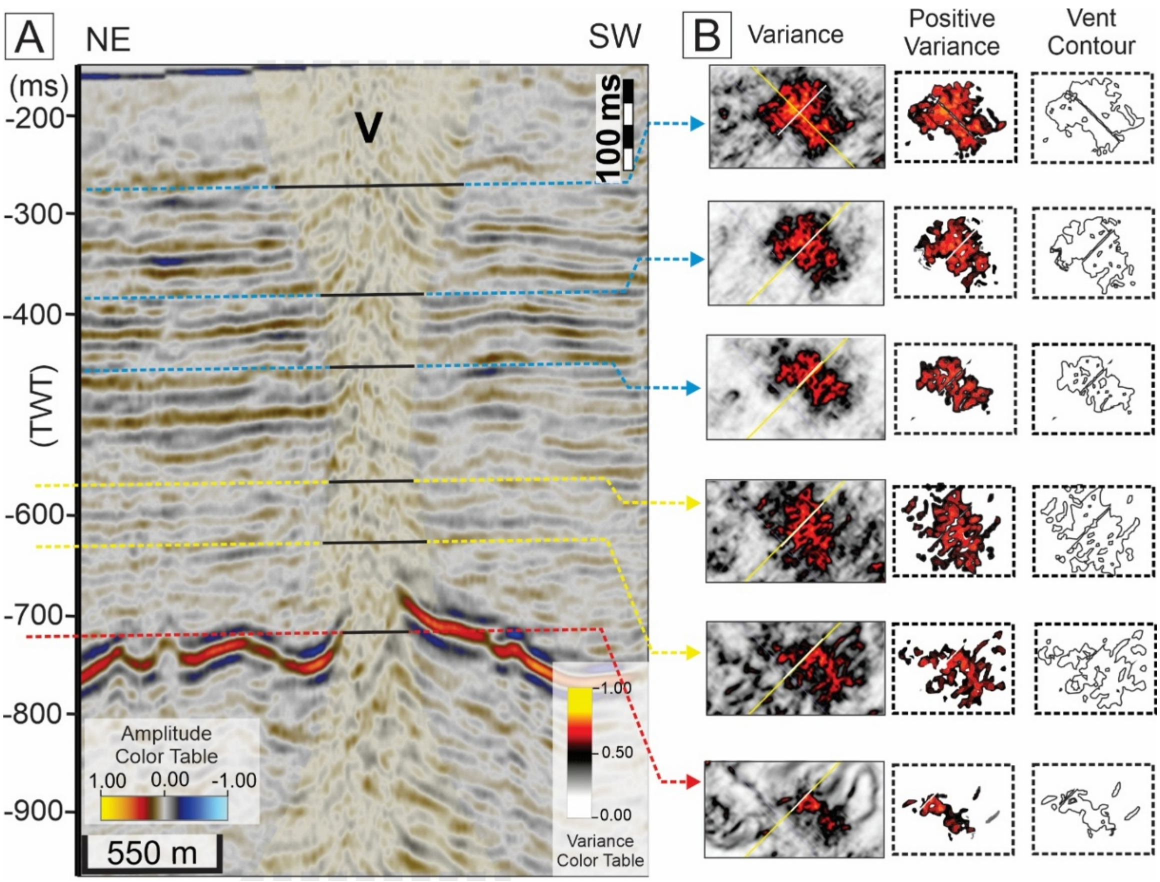

Figure 10. **(A)** Seismic section showing the main measurement points along the geobody, with cuts made at six different depths. The lateral images show the application of the variance attribute, highlighting the influence and control of the Afonso Bezerra Fault on the silicification process. **(B)** Point cloud illustrating how silicification behavior is influenced by fault direction and the boundaries of seismic horizons. Vertical exaggeration: 5x.

Overall, it is possible to observe an increase in the width of the hydrothermal vent in the basement towards the superficial units (Fig. 11). However, each layer has its peculiarities. The analysis of the bar charts shows that the greatest geobody width occurs in the Jandaíra Formation, located in the upper-middle portion of the diagrams. In this unit, the bars frequently exceed 500 m along the horizontal axis, reaching nearly 900 m, indicating wider and laterally continuous bodies. In the Açu Formation, the associated bars display visually smaller and more regular width, generally ranging between 300 and 500 m, with uniform symmetry and shorter horizontal lengths compared to those in Jandaíra. In the crystalline basement, the bars are shorter, exhibiting significantly reduced width, with values typically ranging from 200 to 400 m.

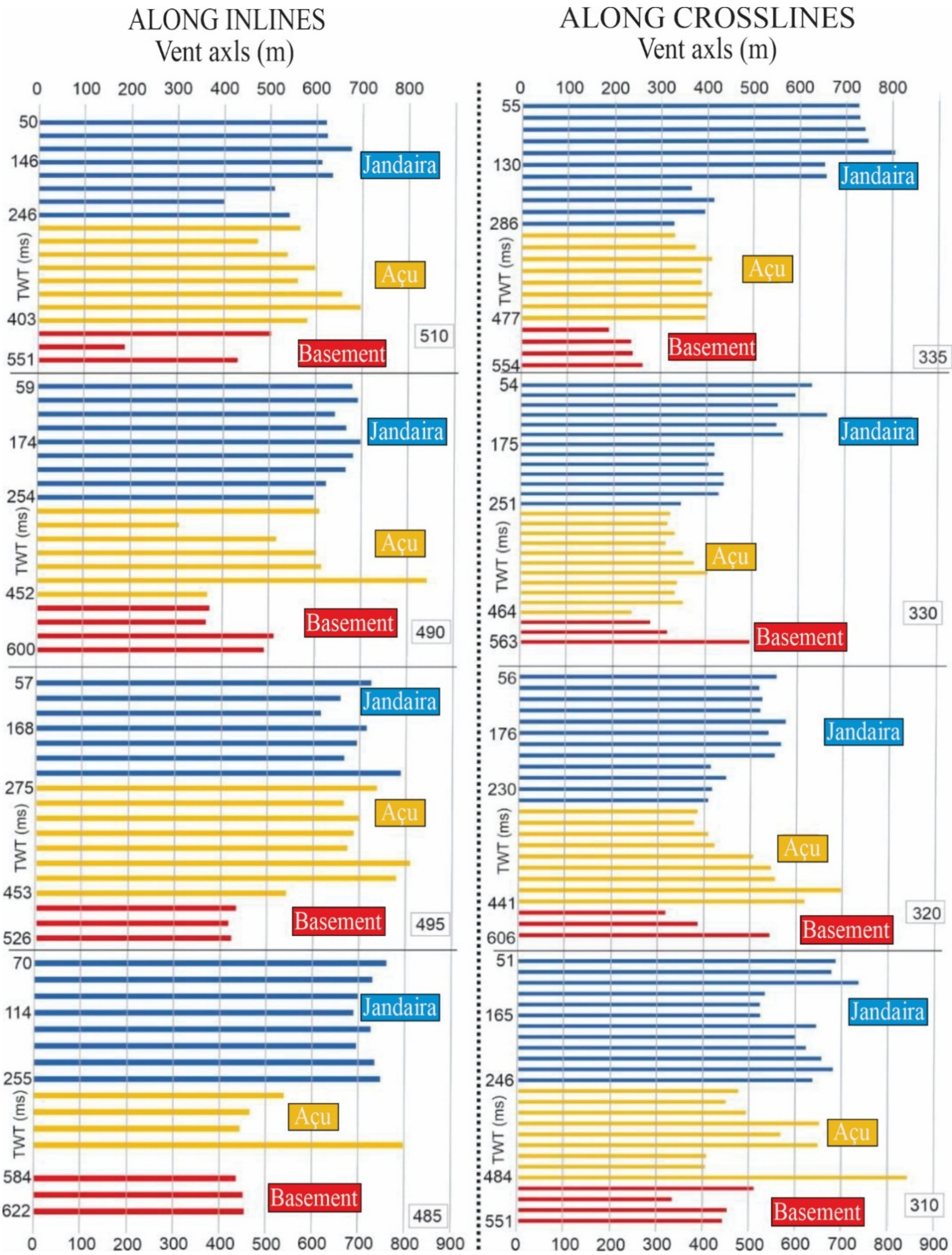

Figure 11. Bar charts showing the lateral width of silicified geobodies along inline (left) and crossline (right) directions in two-way time (TWT, milliseconds). The numbers in the white square correspond to the inline and crossline numbers where measured the lateral width of

silicified geobody.

The details commented on the bar charts (Fig. 11) can be better explored in the scatter plots (Fig. 12). The points corresponding to the Jandaíra Formation (in blue) are concentrated in the upper portions of the vertical axis, with a continuous distribution along the horizontal axis, reaching widths greater than 600 m in some segments. The high density and broad lateral coverage of the points indicate a significant width of silicified bodies in this unit. In the Açu Formation (in yellow), the points are distributed in the intermediate range of the graph, with lateral widths varying between 300 and 500 m along the X-axis. The distribution is more ordered and regular, with less lateral dispersion compared to the Jandaíra. In the crystalline basement (in red), the points are located in the lower portions of the graphs and exhibit a limited lateral extent, with a sparse and discontinuous distribution along the X-axis, generally ranging from 300 to 500 m in width. Additionally, a difference in the trend of measurements can be observed in inlines and crosslines. In inlines, measurements are more dispersed, while in crosslines, there is a clear tendency for basement width to increase for the Jandaíra Formation.

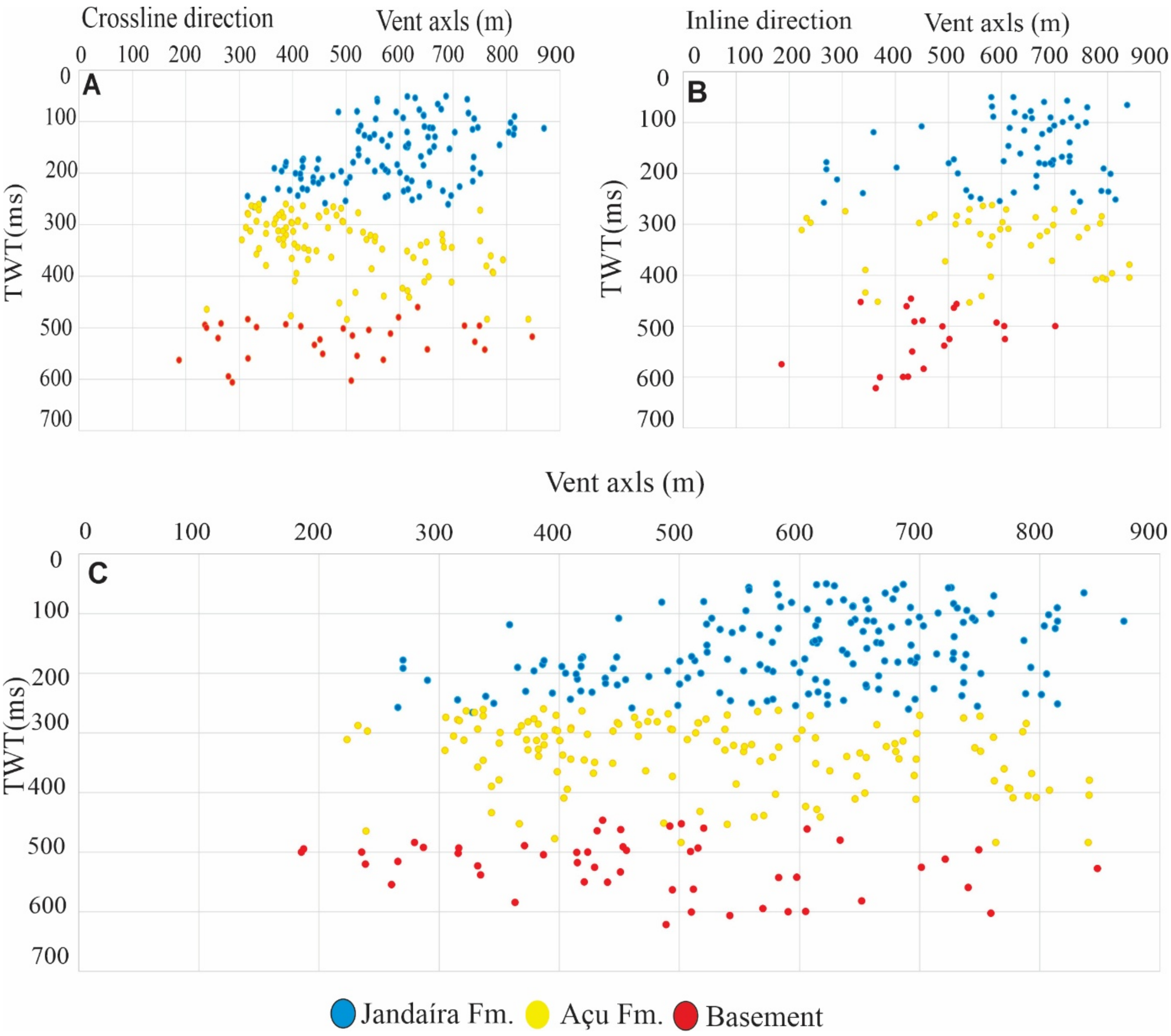

Figure 12. Scatter plots showing the lateral distribution of silicified geobodies by formation. (A) Inline direction, (B) Crossline direction, (C) Combined view.

5. Discussion

5.1. Hydrothermal Silicification Bodies by Seismic Attributes

The gain equalization filter AGC and the variance seismic attribute were crucial for effective discrimination between silicified and non-silicified zones, as well as improved the imaging of the low-amplitude reflectors within the Açu Formation, stratigraphic interfaces, and structural discontinuities that act as primary pathways for silica-rich fluid migration. Although AGC and variance enhanced the detection of subtle seismic features in the Potiguar Basin, the interpretation of complex structures in areas with weak reflectivity (Figs. 4 and 8) remain ambiguous. In such zones, distinguishing between faults and lithological contacts is challenging, as lithological variations can mask smaller-scale faults (Iacopini et al., 2012). Nonetheless, the interpretation is strengthened by surface evidence of hydrothermal silicification, previously documented by Menezes et al. (2019) and Bezerra et al. (2021). These field observations support the identification of the silicified body associated with the ABFS, despite limitations in seismic data quality.

Accurately delineating silicified zones remains a challenge due to lithological heterogeneity where acoustic impedance contrasts are low, as between siliciclastic and carbonate units. Fault zones add further complexity, often displaying discontinuous and irregular patterns that exceed current seismic resolution capabilities (i.e., Liao et al., 2019, 2020). Variance attribute analysis reveals that hydrothermal silicification is not largely pervasive, leaving portions of the host rock unaffected (Fig. 10B), consistent with porosity variations reported in outcrop studies (Menezes et al., 2019). This heterogeneous alteration, which extends from the crystalline basement to shallow stratigraphic levels, underscores the value of integrating seismic attributes with geological interpretation to improve reservoir characterization. In carbonate units like the Jandaíra Formation, the spatial distribution of silicified bodies may indicate structurally connected zones that influence fluid flow and inform optimal well placement. This approach is aligned with the strategies proposed by Basso et al. (2023) for enhanced hydrocarbon exploration efficiency.

5.2. Influence of Host Rock Lithology on Hydrothermal Silicification width

The width of silicified geobodies is directly related to the lithology of the host units. Different rock types respond variably to the silicification process (Menezes et al., 2019; Bezerra et al., 2021; Souza et al., 2021; Palhano et al., 2023). Carbonate units tend to form zones of high porosity and irregular width due to silicification occurring preferentially in fractures and cavities, creating interconnected porous zones. Carbonate rocks are the most affected by width variation, responding significantly to the silicification process by forming heterogeneous zones, including secondary porosity such as vugs and connected fractures (Bezerra et al., 2021; Souza et al., 2021; Basso et al., 2023). This increases internal variability and favors hydraulic connectivity in some regions. In carbonate formations, such as the Jandaíra Formation, greater width are recorded due to the creation of secondary porosity, which facilitates the silicification process (Figs. 11 and 12).

In contrast, siliciclastic rocks generally develop more uniform and compact width with reduced porosity and permeability. Siliciclastic rocks, due to their more homogeneous nature and greater resistance to silica filling, exhibit smaller width variations, which impact the distribution of petrophysical properties to a lesser extent (Palhano et al., 2023; Berio et al., 2025a,b; Rocha et al., 2025). The width of silicified geobodies demonstrates a direct impact on local permeability, varying between lithologies. In siliciclastic rocks, greater width generally act as hydraulic barriers due to silica filling, which drastically reduces pore connectivity (Palhano et al., 2023). This lithological influence creates internal heterogeneity in silicified bodies, which must be considered when interpreting seismic data and reservoir models. The observed width variations are consistent with lithological differences and the structural control exerted by regional faults on hydrothermal fluid circulation. In siliciclastic formations, such as the Açu Formation, silicification occurs in a more restricted manner, resulting in smaller width (Fig. 11), probably due to reduced porous connectivity and greater compaction. These patterns highlight the lithological influence on silicification heterogeneity and its significance to reservoir compartmentalization.

Crystalline rocks are also influenced by silicification, particularly along faults and fractures that act as conduits for hydrothermal fluids (Bezerra et al., 2021). In these zones, the basement may develop local patterns of hydraulic conductivity due to selective silicification in fractures, while compact areas remain impermeable. This behavior highlights the role of tectonic features in channeling fluids, where fault-controlled silicification results in localized zones of increased permeability. The results of this study show that geobodies in the basement exhibit smaller width and shorter bars in the graphs (Fig. 11), indicating a more restricted and localized silicification. Additionally, in the scatter plots (Fig. 12), the segments corresponding to the basement are concentrated in the lower portions of the graph, with low point density and sparse distribution along the lateral axis, reflecting low connectivity and limited lateral propagation. These patterns confirm that silicification in the basement is discrete, discontinuous, and structurally controlled. In terms of width, the silicification observed in the basement aligns more closely with the behavior seen in siliciclastic rocks of the Açu Formation. Both exhibit thinner silicified zones with limited lateral continuity, reflecting a more restricted silicification process (Fig. 12). Furthermore, we observed that the transition surfaces between the units (basement to Açu Formation and Açu Formation to Jandaíra Formation), which are unconformities, did not serve as preferred paths for increasing the width of the hydrothermal flow. Our results generally indicate that these areas exhibit a decrease in the width of the hydrothermal silicification body (Fig. 11). Therefore, our data can be used as input for modeling and numerical simulation of fluid flow, particularly in applications involving the extraction of geobodies from seismic attributes, such as variance.

5.3. Tectonic Influence on Hydrothermal Silicification width

The interaction between the basement and the overlying sedimentary units is crucial, as faults originating in the basement often dictate fluid circulation pathways and influence the structural compartmentalization of formations such as the Açu and Jandaíra Formations. In this study, the seismic interpretation reveals that silicified segments in the basement occur preferentially along fault-controlled zones, aligning spatially with wider and more laterally extensive silicified bodies identified in the overlying formations. This spatial correlation suggests that reactivated basement faults act as vertical conduits for hydrothermal fluids, enabling upward migration and selective silicification in the Açu and Jandaíra units. The geobody depicted in the scatter plots (Fig. 12) demonstrates that, while the basement hosts thin and discontinuous silicified features, the overlying carbonates, particularly in the Jandaíra Formation, record greater width and lateral continuity, consistent with structural focusing of fluid flow along fault corridors. These observations underscore the tectonic inheritance from the basement as a key factor controlling the geometry, width, and distribution of silicification in the sedimentary section.

The basement silicification is highly localized along fault-controlled fractures, suggesting a stronger tectonic influence. Faults and fractures are correlated with the formation of silicified geobodies and act as the main pathways for silica-rich hydrothermal fluid circulation. In the Potiguar Basin, faults such as the ABFS serve as preferential conduits for fluid migration, facilitating silicification along shear zones and fractures (Menezes et al., 2019; Bezerra et al., 2021). This results in heterogeneous width distribution and structural variability of silicification geobodies, which should be considered and integrated into structural models to predict reservoir compartmentalization and connectivity (e.g., Rocha et al., 2025).

In our study, the width variations are more pronounced along seismic directions perpendicular to the main orientations of regional faults (Fig. 12), suggesting that silicification is directly controlled by structural orientation. In directions parallel to the faults, width tends to be more uniform (Fig. 12A), while orthogonal directions (Fig. 12B) highlight zones of greater width, indicating areas of increased hydrothermal fluid circulation. Results from Palhano et al. (2023) support this observation, as their study in the Rio do Peixe Basin demonstrated that silicification was concentrated near fault zones, forming distinct halos of silicified rock with varying degrees of intensity. The intense silicification observed close to the fault core and its gradual reduction away from the fault reflect the influence of fault-controlled fluid pathways. Similarly, the relationship between silicification and structural orientation in this study highlights the importance of integrating tectonic and lithological controls when evaluating reservoir compartmentalization and hydrothermal alteration processes.

6. Conclusions

Integrated seismic interpretation and statistical analysis provided a high-resolution understanding of the structural and stratigraphic controls on hydrothermal silicification in the Potiguar Basin, with a particular emphasis on the Afonso Bezerra Fault System (ABFS). The mapped units — crystalline basement, Alagamar, Açu, and Jandaíra formations — display distinct seismic signatures and play differentiated roles in the migration and accumulation of silica-rich fluids.

The modeling of seismic surfaces revealed the structural architecture of the basement, characterized by horsts and grabens that control the geometry of the overlying sedimentary units. Topographic variations in these surfaces are associated with the structural compartmentalization of the rift system and directly influence the thickening of formations. For instance, the Açu Formation exhibited an almost flat surface, suggesting minimal influence of internal tectonics. At the same time, the basement and the Alagamar Formation exhibited greater structural ruggedness associated with normal fault activity.

The geometric characterization of hydrothermal conduits showed that the identified vents exhibit an "inverted cone" morphology, with roots located below the basement top and direct connections to normal faults that cut through all basin formations. The disturbed zones associated with these conduits are characterized by amplitude attenuation and reflector discontinuities, exhibiting strong lateral contrast compared to adjacent seismic patterns. The use of the AGC gain balancing filter, combined with the variance seismic attribute, proved essential in enhancing the visibility of these features, especially in areas characterized by low signal to noise ratio or limited reflector continuity.

The statistical analysis of silicified geobody width revealed strong lithostratigraphic and structural control on the distribution of silicification. Width was measured in two directions — inline and crossline — allowing for the evaluation of both lateral and vertical variability of the conduits within the seismic volume. Carbonate formations, such as the Jandaíra Formation, showed the highest width values and broad lateral continuity, exceeding 600 meters in some segments. This indicates high hydraulic connectivity, supported by the presence of interconnected vugs and fractures. In contrast, the Açu Formation exhibited intermediate width and a more symmetric distribution, consistent with silica infill in porous layers, though with more limited connectivity. In the basement, silicified geobodies are thin, discontinuous, and confined to fault zones, indicating a tectonic control pattern characterized by localized silicification and limited lateral propagation.

The asymmetry between inline and crossline directions, with greater width aligned parallel to the ABFS trend, reinforces the influence of structural orientation on silicification propagation. In directions orthogonal to the faults, greater variability was observed, suggesting that the faults act as preferential conduits for ascending fluids, controlling both the vertical focus and the lateral distribution of hydrothermal alteration.

Therefore, the distribution of silicification in the study area is not random, but governed by an integrated system of structural inheritance and lithological contrast. The combination of seismic interpretation, advanced attributes, and statistical analysis enabled the identification of zones with greater width, connectivity, and reservoir potential, providing valuable insights for modeling compartmentalization and reservoir quality in tectonically complex settings.

Although the present study has successfully demonstrated the influence of host lithologic units on the width and distribution of the silicified body, certain aspects remain unresolved. Specifically, the role of fault systems in controlling the width of silicification (question iii) and the internal heterogeneity of hydrothermal conduits (question iv) could not be conclusively addressed due to limitations in seismic resolution and data integration. These gaps highlight the need for future studies focused on high-resolution structural interpretation and detailed characterization of fluid migration pathways, which may provide a more comprehensive understanding of the selective nature of hydrothermal silicification.

Acknowledgements

This research was carried out in association with the ongoing R&D project registered as ANP 23505-1, “Processos e Caracterização de Rotas de Fluxo de Fluidos em Reservatórios Carstificados, Fraturados e Silicificados do Pré-Sal – Porocarste Fase II” (UFRN/UNB/UFPE/UFC/UFRA/IFRN/IFPB/Shell Brasil/ANP) – Porokarst Phase II – Processes and Characterization of fluid pathways in Karstified, Fractured and Silicified Reservoirs of the Presalt, sponsored by Shell Brasil under the ANP R&D levy.” Thanks are due to the Brazilian National Council for Scientific and Technological Development (CNPq) for the research fellowships and associated grants to MPG, DLV, FHRB, and WEM.

References

Almeida, F.F.M. de, Hasui, Y., Brito Neves, B.B. de, Fuck, R.A., 1981. Brazilian structural provinces: an introduction. Earth Sci. Rev. 17, 1–29. https://doi.org/10.1016/0012-8252(81)90003-9.

Araque-Pérez, C.J., Teixidó, T., Mancilla, F. de L., Morales, J., 2024. Reprocessing and interpretation of legacy seismic data using machine learning from the Granada Basin, Spain . Tectonophysics , 885, 230414. https://doi.org/10.1016/j.tecto.2024.230414.

Basso, M., Chinelatto, GF, Belila, AMP, Mendes, LC, Souza, JPP, Stefanelli, D., Vidal, AC, & Bueno, JF (2023). Characterization of silicification and dissolution zones by integrating borehole image logs and core samples: A case study of a well from the Brazilian pre-salt. Petroleum Geoscience, 29, [Article 044]. https://doi.org/10.1144/petgeo2022-044.

Berndt, C. (2005). Focused fluid flow in passive continental margins . Philosophical Transactions of the Royal Society A: Mathematical, Physical and Engineering Sciences , 363(1837), 2855–2871. https://doi.org/10.1098/rsta.2005.1666.

Berio, L.R., Balsamo, F., Lucca, A., Pizzati, M., Storti, F., Aldega, L., Cipriani, A., Dallai, L., Lugli, F., Mantovani, L., Moretto, V., Trua, T., Zanchetta, S., Viola, G., 2025a. Hydrothermal silicification and active extensional faulting: Insights from the Kornos-Aghios Ioannis fault, Lemnos Island, Greece. GSA Bull. https://doi.org/10.1130/B37810.1.

Berio, L.R., Bezerra, F.H.R., Brito, M.F.P., Rodrigues, M.A.F., Storti, F., Balsamo, F., 2025b. The impact of hydrothermal silicification on fault zone porosity and permeability: insights from the Kornos-Aghios Ioannis normal fault, Lemnos Island, Greece. J. Struct. Geol. 197, 105444. https://doi.org/10.1016/j.jsg.2025.105444.

Bertani, R.T., Costa, I.G., Matos, R.M.D., 1990. Evolução tectono-sedimentar, estilo estrutural e habitat do petróleo na Bacia Potiguar. In: Gabaglia, G.P.R., Milani, E.J. (Eds.), Origem e evolução de Bacias Sedimentares. Petrobras, Rio de Janeiro, pp. 291-310.

Bertoni, C., Cartwright, J.A.,2005. *3D* seismic analysis of circular evaporite dissolution structures, Eastern Mediterranean . Journal of the Geological Society , 162, 909–926. https://doi.org/10.1144/0016-764904-126.

Bezerra, F.H.R., Ferreira, J.M., Sousa, M.O.L., 2006. Review of seismicity and neogene tectonics in northeastern Brazil. Rev. Asoc . Geol. Argent. 61, 525–535.

Bezerra, F.H.R., Amaral, R.F., Silva, F.O., Sousa, M.O.L., Fonseca, V.P., Vieira, M.M., 2009. Explanatory note for the Macau Sheet (SB.24-XD-II), scale 1:100,000 . Brasilia: Geology of Brazil Program - CPRM/UFRN. ISBN 978-85-7499-035-4.

Bezerra, F.H.R., de Castro, D.L., Maia, R.P., Souza, M.O.L., Moura-Lima, E.N., Rossetti, D.F., Bertotti, G., Souza, Z.S., Nogueira, F.C.C., 2020. Postrift stress field inversion in the Potiguar Basin, Brazil – implications for petroleum systems and evolution of the equatorial margin of South America. Mar. Pet. Geol. 111, 88–104.

Bezerra, F.H., Balsamo, F., Corsi, G., Legrand, J.M., Sousa, M.O.L., Nogueira, F.C.C., Salvioli -Mariani, E., Menezes, C.P., 2021. Hydrothermal silicification in the intraplate Samambaia seismogenic fault, Brazil: Implications for fault loss of cohesion and healing in rifted crust. Tectonophysics, 815, 229002. https://doi.org/10.1016/j.tecto.2021.229002.

Bezerra, F.H.R., Marques, F.O., Vasconcelos, D.L., Rossetti, D.F., Tavares, A.C., Maia, R. P., de Castro, D.L., Nogueira, F.C.C., Medeiros, W.E., 2023. Review of tectonic inversion of sedimentary basins in NE and N Brazil: analysis of mechanisms, timing and effects on structures and relief. J. S. Am. Earth Sci. 126, 104356. https://doi.org/10.1016/j.jsames.2023.104356.

Bjorlykke, K., Egeberg, P.K., 1993. Quartz cementation in sedimentary basins. Am. Assoc. Petrol. Geol. Bull. https://doi.org/10.1306/bdff8ee8-1718-11d7-8645000102c1865d.

Cartwright, J., Santamarina, C. (2015). Seismic characteristics of fluid escape pipes in sedimentary basins: Implications for pipe genesis . Marine and Petroleum Geology , 65, 126-140. https://doi.org/10.1016/j.marpetgeo.2015.03.023.

Catuneanu, O., Galloway, W.E., Kendall, C.G. St. C., Miall, A.D., Posamentier , H.W., Strasser, A., Tucker, M.E., 2011. Sequence stratigraphy: Methodology and nomenclature . Newsletters on Stratigraphy 44(3), 173-245. https://doi.org/10.1127/0078-0421/2011/0011.

Catuneanu, C., 2017. Sequence stratigraphy: guidelines for a standard methodology. Stratigraphy & Timescale 2, 1–57. https://doi.org/10.1016/bs.sats.2017.07.003.

Catuneanu, O. (2019a). Model-independent sequence stratigraphy . Earth-Science Reviews , 188, 312-388. https://doi.org/10.1016/j.earscirev.2018.09.017.

Catuneanu, O. (2019b). Scale in sequence stratigraphy . Marine and Petroleum Geology , 106, 128-159. https://doi.org/10.1016/j.marpetgeo.2019.04.026.

Chen, D., Zhang, G., Wang, X., Wang. Z., Chen, S., Dong, D., 2021. Seismic features and origin of fluid escape pipes offshore Hainan Island on the northern slope of South China Sea. Marine and Petroleum Geology 133, 105276. https://doi.org/10.1016/j.marpetgeo.2021.105276.

Chopra, S., & Marfurt , K. J. (2005). Seismic attributes – A historical perspective . Geophysics, 70(5), 3SO–28SO. https://doi.org/10.1190/1.2098670.

Chopra, S., Marfurt , K.J., 2007. Seismic Attributes for Prospect Identification and Reservoir Characterization. Society of Exploration Geophysicist, p . 481.

Cunha, J.A. de O., Córdoba, V.C., Soares, U.M., Sousa, D.C., Vital, H. 2021. Evolution of shallow and deep-water deposits included in the regressive drift succession of the Potiguar Basin (Brazilian Equatorial Margin) during the Late Cretaceous to Holocene. Journal of South American Earth Sciences, 110, 103420. https://doi.org/10.1016/j.jsames.2021.103420.

Corrêa, R.S.M., Carvalho, B., Ukar, E., Laubach, S.E., Pestilho, A.L.S., Fall, A., Larson, T. Stockli, D., Stockli, L., Lüders, V., Niedermann, S., Banks, D.A., 2025. Brittle deformation and hydrothermal alteration in the Barra Velha Formation, Santos Basin, offshore Brazil. AAPG Bulletin 109, 545-590. https://doi.org/10.1306/03182524012.

Cremonini, O.A. Caracterização Estrutural e Evolução da Área de Ubarana, Porção Submersa da Bacia Potiguar, Brasil. Dissertação de Mestrado – Escola de Minas, Universidade Federal de Ouro Preto. Ouro Preto. 136p. 1993.

Davies, R.J., 2003. Kilometer-scale fluidization structures formed during early burial of a deep-water slope channel on the Niger Delta . Geology 31(11), 949-952. https://doi.org/10.1130/G19835.1.

de Castro, D. L., Bezerra, F. H. R., Sousa, M. O. L., and Fuck, R. A.: Influence of Neoproterozoic tectonic fabric on the origin of the Potiguar Basin, northeastern Brazil and its links with West Africa based on Gravity and Magnetic Data, J. Geodyn., 54, 29 – 42, 2012.

de Castro, D.L. Bezerra, F.H.R., 2015. Fault evolution in the Potiguar rift termination, equatorial margin of Brazil. Solid Earth 6, 185–196. https://doi.org/10.5194/se-6-185-2015.

Fernández-Ibánez, F., Jones, G.D., Mimoun, J.G., Bowen, M.G., Simo, J.A., Marcon, V., Esch, W.L., 2022. Excess permeability in the Brazil pre-Salt: nonmatrix types, concepts, diagnostic indicators, and reservoir implication ns. AAPG Bulletin 106, 701-738. https://doi.org/10.1306/10042120171.

Huuse, M., Mickelson, M., 2004. Eocene sandstone intrusions in the Tampen Spur area (Norwegian North Sea Quad 34) imaged by 3D seismic data. Marine and Petroleum Geology , 21(2), 141–155. https://doi.org/10.1016/j.marpetgeo.2003.11.018.

Huuse, M., Jackson, C.A-L., Van Rensbergen , P., Davies, R.J., Flemings, P.B., Dixon, R.J., 2010. Subsurface sediment remobilization and fluid flow in sedimentary basins: An overview. Basin Research 22(4), 342-360. https://doi.org/10.1111/j.1365-2117.2010.00488.x.

Hustoft, S., Bünz, S., Mienert, J., 2010. Three-dimensional seismic analysis of the morphology and spatial distribution of chimneys beneath the Nyegga pockmark field, offshore mid-Norway. Basin Research 22(4), 465-480. https://doi.org/10.1111/j.1365-2117.2010.00486.x.

Iacopini, D., Butler, R.W.H., Purves, S., 2012. Seismic imaging of thrust faults and structural damage: A visualization workflow for deepwater thrust belts. First Break , 30(5), 39–46. https://doi.org/10.3997/1365-2397.30.5.58681.

Ismail, A., Radwan, A.A., Leila, M., Eysa, E.A., 2024. Integrating 3D subsurface imaging, seismic attributes, and wireline logging analyses: Implications for high-resolution detection of deep-rooted gas escape features, eastern offshore Nile Delta, Egypt. Journal of African Earth Sciences 213, 105230. https://doi.org/10.1016/j.jafrearsci.2024.105230.

Kahrizi, A., Emdadi, M., Karslı, H., 2014. Efficiency of complex trace analysis to attenuate ground-roll noise from seismic data . Journal of Applied Geophysics 106, 50–59. https://doi.org/10.1016/j.jappgeo.2014.04.013.

Karmanov, P., Roy, P.N.S., Reddy, R., 2024. Introduction of new attributes: Scaling Exponent and its double derivatives for better land seismic volume interpretation. Journal of Applied Geophysics 221, 105279. https://doi.org/10.1016/j.jappgeo.2023.105279.

Klimchouk , A. B. (2017). Types and definitions of hypogene karst. In A. Klimchouk et al. (Eds.), *Hypogene karst regions and caves of the world* (pp. 1–39). Springer. https://doi.org/10.1007/978-3-319-53348-3_1.

La Bruna, V., Bezerra, F.H.R., Souza, V.H.P., Maia, R.P., Auler, A.S., Araujo, R.E.B., Cazarin, C.L., Rodrigues, M.A.F., Vieira, L.C., 2021. High-permeability zones in folded and faulted silicified carbonate rocks: Implications for karstified carbonate reservoirs . Marine and Petroleum Geology 128, 105046. https://doi.org/10.1016/j.marpetgeo.2021.105046.

Li, N., Zhang, J., Matsushima, J., Song, C., Luan, X., Dou, M., Chen, T., Wang, L., 2022. Sensitivity analysis of seismic attributes and oil reservoir predictions based on jointing wells and seismic data – A case study in the Taoerhe Sag, China. Frontiers in Marine Science 9, 1011770. https://doi.org/10.3389/fmars.2022.1011770.

Li, N., Matsushima, J., Zhu, X., Song, C., Luan, X., Zhang, J., 2024. Seismic simulation and attribute analysis of Jurassic fluvial reservoirs in the P6 region, Xinjiang. Geoenergy Science and Engineering 233, 212512. https://doi.org/10.1016/j.geoen.2023.212512.

Liao, Z., H. Liu, B. M. Carpenter, K. J. Marfurt, Z. Reches, 2019. Analysis of fault damage zones using three-dimensional seismic coherence in the Anadarko Basin, Oklahoma. AAPG Bulletin 103, 1771–1785. https://doi.org/10.1306/1219181413417207.

Lima, B.E.M., De Ros, L.F., 2019. Deposition, diagenetic and hydrothermal processes in the Aptian Pre-Salt lacustrine carbonate reservoirs of the northern Campos Basin, offshore Brazil. Sedimentary Geology 383, 55–81. https://doi.org/10.1016/j.sedgeo.2019.01.006.

Lima, B.E.M., Tedeschi, L.R., Pestilho, A.L.S., Santos, R.V., Vazquez, J.C., Guzzo, J.V.P., De Ros, L.F., 2020. Deep-burial hydrothermal alteration of the Pre-Salt carbonate reservoirs from northern Campos Basin, offshore Brazil: evidence from petrography, fluid inclusions, Sr, C and O isotopes. Marine and Petroleum Geology 113, 104143. https://doi.org/10.1016/j.marpetgeo.2019.104143.

Lopes, J.A.G., de Castro, D.L., Bertotti, G., 2018. Quantitative analysis of the tectonic subsidence in the Potiguar Basin (NE Brazil). Journal of Geodynamics 117, 60-74. https://doi.org/10.1016/j.jog.2018.04.008.

Løseth, H., Wensaas , L., Arntsen, B., Hanken, N.-M., Basire, C., Graue, K., 2011. 1000 m long gas blow-out pipes. Marine and Petroleum Geology 28(6), 1047–1060. https://doi.org/10.1016/j.marpetgeo.2010.10.001.

Lu, Z., Chen, H., Qing, H., Chi, G., Chen, Q., You, D., Yin, H., Zhang, S. 2017. Petrography, fluid inclusion and isotope studies in Ordovician carbonate reservoirs in the Shunnan area, Tarim basin, NW China: implications for the nature and timing of silicification. Sedimentary Geology 359, 29-43. https://doi.org/10.1016/j.sedgeo.2017.08.002.

Maciel, I.B., Balsamo, F., Bezerra, F.H.R., Nogueira, F.C.C., Berio, L.R., Brod, J.A., Souza, Z.S., Matos-Pimentel, H.L.S., Carvalho, B.R.B.M., Souza, J.A.B., 2024. Hydrothermal silicification along rift border faults in the Rio do Peixe basin, Brazil. Mar. Petrol. Geol. 168,107025. https://doi.org/10.1016/j.marpetgeo.2024.107025.

Maestrelli, D., Iacopini, D., Jihad, A.A., Bond, C.E., Bonini, M., 2017. Seismic and structural characterization of fluid escape pipes using 3D and partial stack seismic from the Loyal Field (Scotland, UK): A multiphase and repeated intrusive mechanism. Marine and Petroleum Geology 88, 489-510. https://doi.org/10.1016/j.marpetgeo.2017.08.016.

Marfurt, K.J., Kirlin, R.L., Farmer, S.L., Bahorich, M.S., 1998. 3-D seismic attributes using a semblance-based coherency algorithm. Geophysics 63(4), 1150-1165. https://doi.org/10.1190/1.1444415.

Matos, R.M.D., 1992. The northeast Brazilian rift system. Tectonics 11 (4), 766–791. https://doi.org/10.1029/91TC03092.

Melo, A.C.C., de Castro, D.L., Bezerra, F.H.R., Bertotti, G., 2016. Rift fault geometry and evolution in the Cretaceous Potiguar Basin (NE Brazil) based on fault growth models. Journal of South American Earth Sciences 71, 96–107. https://doi.org/10.1016/j.jsames.2016.07.006.

Melo, A.H., Magalhães, A.J.C., Menegazzo, M.C., Fragoso, D.G.C., Florencio, C.P., Lima-Filho, F.P., 2021. High-resolution sequence stratigraphy applied for the improvement of hydrocarbon production and reserves: A case study in Cretaceous fluvial deposits of the Potiguar basin, northeast Brazil. Marine and Petroleum Geology 130, 105124. https://doi.org/10.1016/j.marpetgeo.2021.105124.

Menezes, C.P., Bezerra, F.H.R., Balsamo, F., Mozafari, M., Vieira, M.M., Srivastava, N.K., de Castro, D.L., 2019. Hydrothermal silicification along faults affecting carbonate-sandstone units and its impact on reservoir quality, Potiguar Basin, Brazil . Marine and Petroleum Geology 110, 198–217. https://doi.org/10.1016/j.marpetgeo.2019.07.018.

Mitchum Jr., R.M., Vail, P.R., Thompson III., S., 1977a. Seismic stratigraphy and global changes of sea level, Part 2: the depositional sequence as a basic unit for stratigraphic analysis. In: Payton, CE (Ed.), Seismic Stratigraphy – Applications to Hydrocarbon Exploration, vol. 26. Memoir, American Association of Petroleum Geologists, pp. 53–62.

Moss, J.L., Cartwright, J., 2010. 3D seismic expression of km-scale fluid exhaust pipes from offshore Namibia. Basin Research 22(4), 481-501. https://doi.org/10.1111/j.1365-2117.2010.00461.x.

Moura-Lima, E.N., Bezerra, F.H.R., de Castro, D.L. De, Damascena, R.V.C., Vieira, M.M., Legrand, J.M., 2011. Cenozoic reactivation of the system Afonso Bezerra fault system. Geosciences 30, 77–93.

Nanda, N.C., 2016. Seismic Data Interpretation and Evaluation for Hydrocarbon Exploration and Production: A Practitioner's Guide . Springer International Publishing. ISBN 978-3-319-26489-9. doi : 10.1007/978-3-319-26491-2.

Nasıf, A., 2024. Processing and joint interpretation of multi-resolution marine seismic datasets. Journal of Applied Geophysics 227, 105429. https://doi.org/10.1016/j.jappgeo.2024.105429.

Ngwenya, B.T., Elphick, S.C., Main, I.G., Shimmield, G.B., 2000. Experimental constraints on the diagenetic self-sealing capacity of faults in high porosity rocks. Earth Planet Sci. Lett. 183, 187–199. https://doi.org/10.1016/S0012-821X(00)00261-2.

Oliveira, L.S., Alaei, B., Torabi, A., Oliveira, K.M., Vasconcelos, D.L., Bezerra, F.H.R., Nogueira, F.C.C., 2023. Automatic 3D fault detection and characterization — A comparison between seismic attribute methods and deep learning . Interpretation 11(4), 1–16. https://doi.org/10.1190/int-2023-0016.1.

Palhano, L.C., Nogueira, F.C.C., Marques, F.O., Vasconcelos, D.L., Bezerra, F.H., Souza, J.A.B., Nicchio, M.A., Balsamo, F., 2023. Influence of hydrothermal silicification on the physical properties of a basin-boundary fault affecting arkosic porous sandstones, Rio do Peixe Basin, Brazil . Marine and Petroleum Geology 148, 106062. https://doi.org/10.1016/j.marpetgeo.2022.106062.

Pang, H.-W., Wang, H.-Q., Xiao, Y.-T., Jin, Y., Lu, Y.-H., Fan, Y.-D., Nie, Z., 2024. Machine learning for carbonate formation drilling: Mud loss prediction using seismic attributes and mud loss records. Petroleum Science 21, 1241–1256. https://doi.org/10.1016/j.petsci.2023.10.024.

Pessoa Neto, O.C., Soares, U.M., Silva, J.G.F., Roesner, E.H., Florencio, C.P., Souza, C.A.V., 2007. Potiguar Basin . Petrobras Geosciences Bulletin 15(2), 357-369. Available at: https://bgp.petrobras.com.br/bgp/article/view/326.

Posamentier , H.W., Kolla, V., 2003. Seismic geomorphology and stratigraphy of depositional elements in deep-water settings. J. Sediment. Res. 73 (3), 367–388. https://doi.org/10.1306/111302730367.

Rocha, R.N.R., Nogueira, F.C.C., Pontes, C.C.C., Gomes, T.P.L., Vasconcelos, D.L., Palhano, L.C., Souza, J.A.B., Perez, Y.A.R., Nicchio, M.A., 2025. 3D modeling and fluid flow simulations along fault zone affected by silicification in Rio do Peixe Basin, Brazil. Journal of South American Earth Sciences 161, 105574. https://doi.org/10.1016/j.jsames.2025.105574.

Souza, V.H.P., Bezerra, F.H.R., Vieira, L.C., Cazarin, C.L., Brod, J.A., 2021. Hydrothermal silicification confined to stratigraphic layers: Implications for carbonate reservoirs. *Marine and Petroleum Geology 124, 104818*. https://doi.org/10.1016/j.marpetgeo.2020.104818.

Strugale, M., Lima, B.E.M., Day, C., Omma, J., Rushton, J., Olivito, J.P.R., Bouch, J., Robb, L., Roberts, N., Cartwright, J., 2024. Diagenetic products, settings and evolution of the pre-salt succession in the Northern Campos Basin, Brazil Geol. Soc. London, Spec. Publ. 548. https://doi.org/10.1144/sp548-2023-93.

Yilmaz, O., 2001. Seismic Data Analysis: Processing, Inversion, and Interpretation of Seismic Data . Society of Exploration Geophysicists, Tulsa, OK, 2027 pp. https://doi.org/10.1190/1.9781560801580.

You D., Han, J., Hu, W., Qian, Y., Chen, Q., Xi, B., Ma, H. 2018. Characteristics and formation mechanisms of silicified carbonate reservoirs in well SN4 of the Tarim Basin. Energy

Exploration & Exploitation 36, 820-849. https://doi.org/10.1177/0144598718757515.

Figure captions

Figure 1. (A) The South American Continent and the location of the Potiguar Basin. (B) Location map of the Potiguar Basin in northeastern Brazil. Modified from Bertani et al. (1990), Bezerra et al. (2009), and de Castro and Bezerra (2015). The Afonso Bezerra Fault System is marked in bold and the study area. (C) Geological-structural map of the study area showing the dataset, including a 3D seismic cube, 2D seismic lines, geobody, and wells used for lithostratigraphic correlation The features used in this map are based on Bezerra et al. (2009).

Figure 2. Simplified stratigraphic column of the Potiguar Basin, showing the main formations from the rift, post-rift, and drift phases, as well as the underlying crystalline basement units. The Alagamar, Açu, and Jandaíra formations represent the key units analyzed in this study. Modified from Pessoa Neto et al. (2007) and Cunha et al. (2021).

Figure 3. (A) Uninterpreted and (B) interpreted 2D seismic section with lithostratigraphic correlation based on Well 1, identifying four main units: Basement, Pendência Formation, Açu Formation, and Jandaíra Formation. See Fig. 1C for the location of this section. Vertical exaggeration: 5x.

Figure 4. (A) Uninterpreted and (B) interpreted seismic section from the seismic volume with stratigraphic correlation based on Well 2, identifying four main units: Basement, Alagamar Formation, Açu Formation, and Jandaíra Formation. Unit boundaries are defined by distinct reflectors, with seismic facies variations observed as depth increases. See Fig. 1C for the location of this section. Vertical exaggeration: 5x.

Figure 5. Stratigraphic interpretation based on seismic reflector patterns, identifying the top of the crystalline basement, the Alagamar Formation, the Açu Formation, and the Jandaíra

Formation, based on the seismic volume data.

Figure 6. Seismic surfaces in TWT. (A) Açu Formation top. (B) Alagamar Formation top. (C) Basement top. The black dashed lines in A and C, and the white dashed line in C are related to the location of the hydrothermal silicification vent. Vertical exaggeration: 5x.

Figure 7. Interpreted seismic section showing the crystalline basement and the overlying Alagamar, Açu, and Jandaíra formations. The image highlights variations in seismic facies, reflector continuity, and stratigraphic boundaries throughout the section. The seismic sections are located in Figure 6(A,B and C). Vertical exaggeration: 5×.

Figure 8. Seismic sections illustrate the geometry of hydrothermal vents. (A) Vents marked by disturbed zones (DZ) with disrupted reflectors and amplitude attenuation. The root zone lies below the top of the basement. (B) Vents connected to the fluid source unit by normal faults, showing the upward pathway of hydrothermal fluids through the basin formations. Vertical exaggeration: 5x. The seismic sections correspond to the geobody depicted in Figure 1C and are located in Figure 6A.

Figure 9. *(A)* Interpreted seismic section with Automatic Gain Control (AGC) applied, showing hydrothermal vent cutting through the Basement, Açu Formation, and Jandaíra Formation. *(B)* Variance attribute applied to the same section, highlighting structural discontinuities associated with the vent, revealing the internal geometry and lateral boundaries of the disturbed zone. Vertical exaggeration: 5x. The seismic section correspond to the geobody depicted in Figure 1C and is located in Figure 6C.

Figure 10. **(A)** Seismic section showing the main measurement points along the geobody, with cuts made at six different depths. The lateral images show the application of the variance attribute, highlighting the influence and control of the Afonso Bezerra Fault on the silicification

process. **(B)** Point cloud illustrating how silicification behavior is influenced by fault direction and the boundaries of seismic horizons. Vertical exaggeration: 5x.

Figure 11. Bar charts showing the lateral width of silicified geobodies along inline (left) and crossline (right) directions in two-way time (TWT, milliseconds). The numbers in the white square correspond to the inline and crossline numbers where measured the lateral width of silicified geobodies.

Figure 12. Scatter plots showing the lateral distribution of silicified geobodies by formation. (A) Inline direction, (B) Crossline direction, (C) Combined view.

Table captions

Table 1. Statistical summary of depth (TWT) and width (m) for the analyzed silicified geobody (time-depth calibrations were based on well-to-seismic ties using checkshot data). The data is presented separately for crosslines and inlines, showing key measures of central tendency (median and mean), variability (standard deviation), and range (maximum and minimum) for the seismic attributes. This analysis highlights the spatial variability and provides insights into the distribution of silicification in the study area.

Capítulo 5. Considerações Finais

5. CONSIDERAÇÕES FINAIS

Este estudo demonstrou a eficácia da integração entre interpretação sísmica, realce de sinal e análise estatística, com vistas à caracterização da silicificação hidrotermal ao longo do Sistema de Falhas Afonso Bezerra (SFAB), na Bacia Potiguar. A metodologia adotada permitiu interpretar, com alta resolução, os controles estratigráficos e estruturais sobre a migração e o aprisionamento de fluidos ricos em sílica.

A aplicação do filtro de ganho equalizador (AGC) e do atributo de variância aos dados sísmicos 2D e 3D foi fundamental para identificar condutos verticais, zonas fraturadas e compartimentos estruturais com distintos padrões de silicificação. O AGC aumentou a visibilidade de refletores profundos e de baixa amplitude, enquanto a variância realçou descontinuidades laterais e zonas perturbadas, associadas a estruturas do tipo vent, contribuindo para a delimitação da geometria interna do corpo silicificado.

Os resultados revelaram que a espessura e a continuidade lateral da silicificação variam conforme a unidade litológica. Na Formação Jandaíra, o corpo geológico silicificado apresenta maior espessura e continuidade, favorecidos por porosidade secundária. Na Formação Açu, a silicificação é mais delgada e homogênea, atuando como barreira ao fluxo. No embasamento, o corpo concentra-se nas zonas de falha, reforçando o papel das estruturas na condução vertical dos fluidos.

A análise estatística da espessura mostrou correlação direta com a litologia e a orientação das falhas, indicando que os contrastes estratigráficos e a compartimentação estrutural controlam a geometria e a conectividade da silicificação. Esses resultados contribuem para a compreensão de sistemas hidrotermais em bacias rifteadas e para o aperfeiçoamento de modelos geológicos de reservatórios fraturados e silicificados.

Recomenda-se a aplicação da abordagem integrada utilizada neste trabalho em áreas com diferentes contextos tectono estratigráficos. A incorporação de atributos sísmicos adicionais, modelagem geológica tridimensional, dados petrofísicos e aerofotogramétricos de alta resolução pode ampliar a interpretação de zonas de fluxo e a avaliação da conectividade hidráulica, contribuindo para o avanço de modelos preditivos em sistemas silicificados.

Embora o presente estudo tenha demonstrado, com êxito, a influência das unidades litológicas hospedeiras sobre a largura e a distribuição do corpo silicificado, certos aspectos permanecem sem elucidação definitiva. Especificamente, o papel dos sistemas de falhas no controle da largura da silicificação (questão iii) e a heterogeneidade interna dos condutos hidrotermais (questão iv) não puderam ser analisados de forma conclusiva, devido a limitações na resolução sísmica e na integração de dados. Essas lacunas ressaltam a necessidade de estudos futuros direcionados à interpretação estrutural em alta resolução e à caracterização detalhada das rotas de migração de fluidos, os quais poderão fornecer uma compreensão mais aprofundada da natureza seletiva da silicificação hidrotermal.

Referências

Referências

Almeida, F.F.M. de, Hasui, Y., Brito Neves, B.B. de, Fuck, R.A., 1981. Brazilian structural provinces: an introduction. Earth Sci. Rev. 17, 1–29. https://doi.org/10.1016/0012-8252(81)90003-9.

Araque-Pérez, C.J., Teixidó, T., Mancilla, F. de L., Morales, J., 2024. Reprocessing and interpretation of legacy seismic data using machine learning from the Granada Basin, Spain . Tectonophysics , 885, 230414. https://doi.org/10.1016/j.tecto.2024.230414.

Basso, M., Chinelatto, GF, Belila, AMP, Mendes, LC, Souza, JPP, Stefanelli, D., Vidal, AC, & Bueno, JF (2023). Characterization of silicification and dissolution zones by integrating borehole image logs and core samples: A case study of a well from the Brazilian pre-salt. Petroleum Geoscience, 29, [Article 044]. https://doi.org/10.1144/petgeo2022-044.

Berndt, C. (2005). Focused fluid flow in passive continental margins . Philosophical Transactions of the Royal Society A: Mathematical, Physical and Engineering Sciences , 363(1837), 2855–2871. https://doi.org/10.1098/rsta.2005.1666.

Berio, L.R., Balsamo, F., Lucca, A., Pizzati, M., Storti, F., Aldega, L., Cipriani, A., Dallai, L., Lugli, F., Mantovani, L., Moretto, V., Trua, T., Zanchetta, S., Viola, G., 2025a. Hydrothermal silicification and active extensional faulting: Insights from the Kornos-Aghios Ioannis fault, Lemnos Island, Greece. GSA Bull. https://doi.org/10.1130/B37810.1.

Berio, L.R., Bezerra, F.H.R., Brito, M.F.P., Rodrigues, M.A.F., Storti, F., Balsamo, F., 2025b. The impact of hydrothermal silicification on fault zone porosity and permeability: insights from the Kornos-Aghios Ioannis normal fault, Lemnos Island, Greece. J. Struct. Geol. 197, 105444. https://doi.org/10.1016/j.jsg.2025.105444.

Bertani, R.T., Costa, I.G., Matos, R.M.D., 1990. Evolução tectono-sedimentar, estilo estrutural e habitat do petróleo na Bacia Potiguar. In: Gabaglia, G.P.R., Milani, E.J. (Eds.), Origem e evolução de Bacias Sedimentares. Petrobras, Rio de Janeiro, pp. 291-310.

Bertoni, C., Cartwright, J.A.,2005. *3D* seismic analysis of circular evaporite dissolution structures, Eastern Mediterranean . Journal of the Geological Society , 162, 909–926. https://doi.org/10.1144/0016-764904-126.

Bezerra, F.H.R., Ferreira, J.M., Sousa, M.O.L., 2006. Review of seismicity and neogene tectonics in northeastern Brazil. Rev. Asoc . Geol. Argent. 61, 525–535.

Bezerra, F.H.R., Amaral, R.F., Silva, F.O., Sousa, M.O.L., Fonseca, V.P., Vieira, M.M., 2009. Explanatory note for the Macau Sheet (SB.24-XD-II), scale 1:100,000 . Brasilia: Geology of Brazil Program - CPRM/UFRN. ISBN 978-85-7499-035-4.

Bezerra, F.H.R., de Castro, D.L., Maia, R.P., Souza, M.O.L., Moura-Lima, E.N., Rossetti, D.F., Bertotti, G., Souza, Z.S., Nogueira, F.C.C., 2020. Postrift stress field inversion in the Potiguar Basin, Brazil – implications for petroleum systems and evolution of the equatorial margin of South America. Mar. Pet. Geol. 111, 88–104.

Bezerra, F.H., Balsamo, F., Corsi, G., Legrand, J.M., Sousa, M.O.L., Nogueira, F.C.C., Salvioli -Mariani, E., Menezes, C.P., 2021. Hydrothermal silicification in the intraplate Samambaia seismogenic fault, Brazil: Implications for fault loss of cohesion and healing in rifted crust. Tectonophysics, 815, 229002. https://doi.org/10.1016/j.tecto.2021.229002.

Bezerra, F.H.R., Marques, F.O., Vasconcelos, D.L., Rossetti, D.F., Tavares, A.C., Maia, R. P., de Castro, D.L., Nogueira, F.C.C., Medeiros, W.E., 2023. Review of tectonic inversion of sedimentary basins in NE and N Brazil: analysis of mechanisms, timing and effects on structures and relief. J. S. Am. Earth Sci. 126, 104356. https://doi.org/10.1016/j.jsames.2023.104356.

Bjorlykke, K., Egeberg, P.K., 1993. Quartz cementation in sedimentary basins. Am. Assoc. Petrol. Geol. Bull. https://doi.org/10.1306/bdff8ee8-1718-11d7-8645000102c1865d.

Cartwright, J., Santamarina, C. (2015). Seismic characteristics of fluid escape pipes in sedimentary basins: Implications for pipe genesis . Marine and Petroleum Geology , 65, 126-140. https://doi.org/10.1016/j.marpetgeo.2015.03.023.

Catuneanu, O., Galloway, W.E., Kendall, C.G. St. C., Miall, A.D., Posamentier , H.W., Strasser, A., Tucker, M.E., 2011. Sequence stratigraphy: Methodology and nomenclature . Newsletters on Stratigraphy 44(3), 173-245. https://doi.org/10.1127/0078-0421/2011/0011.

Catuneanu, C., 2017. Sequence stratigraphy: guidelines for a standard methodology. Stratigraphy & Timescale 2, 1–57. https://doi.org/10.1016/bs.sats.2017.07.003.

Catuneanu, O. (2019a). Model-independent sequence stratigraphy . Earth-Science Reviews , 188, 312-388. https://doi.org/10.1016/j.earscirev.2018.09.017.

Catuneanu, O. (2019b). Scale in sequence stratigraphy . Marine and Petroleum Geology , 106, 128-159. https://doi.org/10.1016/j.marpetgeo.2019.04.026.

Chen, D., Zhang, G., Wang, X., Wang. Z., Chen, S., Dong, D., 2021. Seismic features and origin of fluid escape pipes offshore Hainan Island on the northern slope of South China Sea. Marine and Petroleum Geology 133, 105276. https://doi.org/10.1016/j.marpetgeo.2021.105276.

Chopra, S., & Marfurt , K. J. (2005). Seismic attributes – A historical perspective . Geophysics, 70(5), 3SO–28SO. https://doi.org/10.1190/1.2098670.

Chopra, S., Marfurt , K.J., 2007. Seismic Attributes for Prospect Identification and Reservoir Characterization. Society of Exploration Geophysicist, p . 481.

Cunha, J.A. de O., Córdoba, V.C., Soares, U.M., Sousa, D.C., Vital, H. 2021. Evolution of shallow and deep-water deposits included in the regressive drift succession of the Potiguar Basin (Brazilian Equatorial Margin) during the Late Cretaceous to Holocene. Journal of South American Earth Sciences, 110, 103420. https://doi.org/10.1016/j.jsames.2021.103420.

Corrêa, R.S.M., Carvalho, B., Ukar, E., Laubach, S.E., Pestilho, A.L.S., Fall, A., Larson, T. Stockli, D., Stockli, L., Lüders, V., Niedermann, S., Banks, D.A., 2025. Brittle deformation and hydrothermal alteration in the Barra Velha Formation, Santos Basin, offshore Brazil. AAPG

Bulletin 109, 545-590. https://doi.org/10.1306/03182524012.

Cremonini, O.A. Caracterização Estrutural e Evolução da Área de Ubarana, Porção Submersa da Bacia Potiguar, Brasil. Dissertação de Mestrado – Escola de Minas, Universidade Federal de Ouro Preto. Ouro Preto. 136p. 1993.

Davies, R.J., 2003. Kilometer-scale fluidization structures formed during early burial of a deep-water slope channel on the Niger Delta . Geology 31(11), 949-952. https://doi.org/10.1130/G19835.1.

de Castro, D. L., Bezerra, F. H. R., Sousa, M. O. L., and Fuck, R. A.: Influence of Neoproterozoic tectonic fabric on the origin of the Potiguar Basin, northeastern Brazil and its links with West Africa based on Gravity and Magnetic Data, J. Geodyn., 54, 29 – 42, 2012.

de Castro, D.L. Bezerra, F.H.R., 2015. Fault evolution in the Potiguar rift termination, equatorial margin of Brazil. Solid Earth 6, 185–196. https://doi.org/10.5194/se-6-185-2015.

Fernández-Ibánez, F., Jones, G.D., Mimoun, J.G., Bowen, M.G., Simo, J.A., Marcon, V., Esch, W.L., 2022. Excess permeability in the Brazil pre-Salt: nonmatrix types, concepts, diagnostic indicators, and reservoir implication ns. AAPG Bulletin 106, 701-738. https://doi.org/10.1306/10042120171.

Huuse, M., Mickelson, M., 2004. Eocene sandstone intrusions in the Tampen Spur area (Norwegian North Sea Quad 34) imaged by 3D seismic data. Marine and Petroleum Geology , 21(2), 141–155. https://doi.org/10.1016/j.marpetgeo.2003.11.018.

Huuse, M., Jackson, C.A-L., Van Rensbergen , P., Davies, R.J., Flemings, P.B., Dixon, R.J., 2010. Subsurface sediment remobilization and fluid flow in sedimentary basins: An overview. Basin Research 22(4), 342-360. https://doi.org/10.1111/j.1365-2117.2010.00488.x.

Hustoft, S., Bünz, S., Mienert, J., 2010. Three-dimensional seismic analysis of the morphology and spatial distribution of chimneys beneath the Nyegga pockmark field, offshore mid-Norway. Basin Research 22(4), 465-480. https://doi.org/10.1111/j.1365-2117.2010.00486.x.

Iacopini, D., Butler, R.W.H., Purves, S., 2012. Seismic imaging of thrust faults and structural damage: A visualization workflow for deepwater thrust belts. First Break , 30(5), 39–46. https://doi.org/10.3997/1365-2397.30.5.58681.

Ismail, A., Radwan, A.A., Leila, M., Eysa, E.A., 2024. Integrating 3D subsurface imaging, seismic attributes, and wireline logging analyses: Implications for high-resolution detection of deep-rooted gas escape features, eastern offshore Nile Delta, Egypt. Journal of African Earth Sciences 213, 105230. https://doi.org/10.1016/j.jafrearsci.2024.105230.

Kahrizi, A., Emdadi, M., Karslı, H., 2014. Efficiency of complex trace analysis to attenuate ground-roll noise from seismic data . Journal of Applied Geophysics 106, 50–59. https://doi.org/10.1016/j.jappgeo.2014.04.013.

Karmanov, P., Roy, P.N.S., Reddy, R., 2024. Introduction of new attributes: Scaling Exponent and its double derivatives for better land seismic volume interpretation. Journal of Applied Geophysics 221, 105279. https://doi.org/10.1016/j.jappgeo.2023.105279.

Klimchouk , A. B. (2017). Types and definitions of hypogene karst. In A. Klimchouk et al. (Eds.), *Hypogene karst regions and caves of the world* (pp. 1–39). Springer. https://doi.org/10.1007/978-3-319-53348-3_1.

La Bruna, V., Bezerra, F.H.R., Souza, V.H.P., Maia, R.P., Auler, A.S., Araujo, R.E.B., Cazarin, C.L., Rodrigues, M.A.F., Vieira, L.C., 2021. High-permeability zones in folded and faulted silicified carbonate rocks: Implications for karstified carbonate reservoirs . Marine and Petroleum Geology 128, 105046. https://doi.org/10.1016/j.marpetgeo.2021.105046.

Li, N., Zhang, J., Matsushima, J., Song, C., Luan, X., Dou, M., Chen, T., Wang, L., 2022. Sensitivity analysis of seismic attributes and oil reservoir predictions based on jointing wells and seismic data – A case study in the Taoerhe Sag, China. Frontiers in Marine Science 9, 1011770. https://doi.org/10.3389/fmars.2022.1011770.

Li, N., Matsushima, J., Zhu, X., Song, C., Luan, X., Zhang, J., 2024. Seismic simulation and attribute analysis of Jurassic fluvial reservoirs in the P6 region, Xinjiang. Geoenergy Science and Engineering 233, 212512. https://doi.org/10.1016/j.geoen.2023.212512.

Liao, Z., H. Liu, B. M. Carpenter, K. J. Marfurt, Z. Reches, 2019. Analysis of fault damage zones using three-dimensional seismic coherence in the Anadarko Basin, Oklahoma. AAPG Bulletin 103, 1771–1785. https://doi.org/10.1306/1219181413417207.

Lima, B.E.M., De Ros, L.F., 2019. Deposition, diagenetic and hydrothermal processes in the Aptian Pre-Salt lacustrine carbonate reservoirs of the northern Campos Basin, offshore Brazil. Sedimentary Geology 383, 55–81. https://doi.org/10.1016/j.sedgeo.2019.01.006.

Lima, B.E.M., Tedeschi, L.R., Pestilho, A.L.S., Santos, R.V., Vazquez, J.C., Guzzo, J.V.P., De Ros, L.F., 2020. Deep-burial hydrothermal alteration of the Pre-Salt carbonate reservoirs from northern Campos Basin, offshore Brazil: evidence from petrography, fluid inclusions, Sr, C and O isotopes. Marine and Petroleum Geology 113, 104143. https://doi.org/10.1016/j.marpetgeo.2019.104143.

Lopes, J.A.G., de Castro, D.L., Bertotti, G., 2018. Quantitative analysis of the tectonic subsidence in the Potiguar Basin (NE Brazil). Journal of Geodynamics 117, 60-74. https://doi.org/10.1016/j.jog.2018.04.008.

Løseth, H., Wensaas , L., Arntsen, B., Hanken, N.-M., Basire, C., Graue, K., 2011. 1000 m long gas blow-out pipes. Marine and Petroleum Geology 28(6), 1047–1060. https://doi.org/10.1016/j.marpetgeo.2010.10.001.

Lu, Z., Chen, H., Qing, H., Chi, G., Chen, Q., You, D., Yin, H., Zhang, S. 2017. Petrography, fluid inclusion and isotope studies in Ordovician carbonate reservoirs in the Shunnan area, Tarim basin, NW China: implications for the nature and timing of silicification. Sedimentary Geology 359, 29-43. https://doi.org/10.1016/j.sedgeo.2017.08.002.

Maciel, I.B., Balsamo, F., Bezerra, F.H.R., Nogueira, F.C.C., Berio, L.R., Brod, J.A., Souza, Z.S., Matos-Pimentel, H.L.S., Carvalho, B.R.B.M., Souza, J.A.B., 2024. Hydrothermal silicification along rift border faults in the Rio do Peixe basin, Brazil. Mar. Petrol. Geol.

168,107025. https://doi.org/10.1016/j.marpetgeo.2024.107025.

Maestrelli, D., Iacopini, D., Jihad, A.A., Bond, C.E., Bonini, M., 2017. Seismic and structural characterization of fluid escape pipes using 3D and partial stack seismic from the Loyal Field (Scotland, UK): A multiphase and repeated intrusive mechanism. Marine and Petroleum Geology 88, 489-510. https://doi.org/10.1016/j.marpetgeo.2017.08.016.

Marfurt, K.J., Kirlin, R.L., Farmer, S.L., Bahorich, M.S., 1998. 3-D seismic attributes using a semblance-based coherency algorithm. Geophysics 63(4), 1150-1165. https://doi.org/10.1190/1.1444415.

Matos, R.M.D., 1992. The northeast Brazilian rift system. Tectonics 11 (4), 766–791. https://doi.org/10.1029/91TC03092.

Melo, A.C.C., de Castro, D.L., Bezerra, F.H.R., Bertotti, G., 2016. Rift fault geometry and evolution in the Cretaceous Potiguar Basin (NE Brazil) based on fault growth models. Journal of South American Earth Sciences 71, 96–107. https://doi.org/10.1016/j.jsames.2016.07.006.

Melo, A.H., Magalhães, A.J.C., Menegazzo, M.C., Fragoso, D.G.C., Florencio, C.P., Lima-Filho, F.P., 2021. High-resolution sequence stratigraphy applied for the improvement of hydrocarbon production and reserves: A case study in Cretaceous fluvial deposits of the Potiguar basin, northeast Brazil. Marine and Petroleum Geology 130, 105124. https://doi.org/10.1016/j.marpetgeo.2021.105124.

Menezes, C.P., Bezerra, F.H.R., Balsamo, F., Mozafari, M., Vieira, M.M., Srivastava, N.K., de Castro, D.L., 2019. Hydrothermal silicification along faults affecting carbonate-sandstone units and its impact on reservoir quality, Potiguar Basin, Brazil . Marine and Petroleum Geology 110, 198–217. https://doi.org/10.1016/j.marpetgeo.2019.07.018.

Mitchum Jr., R.M., Vail, P.R., Thompson III., S., 1977a. Seismic stratigraphy and global changes of sea level, Part 2: the depositional sequence as a basic unit for stratigraphic analysis. In: Payton, CE (Ed.), Seismic Stratigraphy – Applications to Hydrocarbon Exploration, vol. 26. Memoir, American Association of Petroleum Geologists, pp. 53–62.

Moss, J.L., Cartwright, J., 2010. 3D seismic expression of km-scale fluid exhaust pipes from offshore Namibia. Basin Research 22(4), 481-501. https://doi.org/10.1111/j.1365-2117.2010.00461.x.

Moura-Lima, E.N., Bezerra, F.H.R., de Castro, D.L. De, Damascena, R.V.C., Vieira, M.M., Legrand, J.M., 2011. Cenozoic reactivation of the system Afonso Bezerra fault system. Geosciences 30, 77–93.

Nanda, N.C., 2016. Seismic Data Interpretation and Evaluation for Hydrocarbon Exploration and Production: A Practitioner's Guide . Springer International Publishing. ISBN 978-3-319-26489-9. doi : 10.1007/978-3-319-26491-2.

Nasıf, A., 2024. Processing and joint interpretation of multi-resolution marine seismic datasets. Journal of Applied Geophysics 227, 105429. https://doi.org/10.1016/j.jappgeo.2024.105429.

Ngwenya, B.T., Elphick, S.C., Main, I.G., Shimmield, G.B., 2000. Experimental constraints on the diagenetic self-sealing capacity of faults in high porosity rocks. Earth Planet Sci. Lett. 183, 187–199. https://doi.org/10.1016/S0012-821X(00)00261-2.

Oliveira, L.S., Alaei, B., Torabi, A., Oliveira, K.M., Vasconcelos, D.L., Bezerra, F.H.R., Nogueira, F.C.C., 2023. Automatic 3D fault detection and characterization — A comparison between seismic attribute methods and deep learning . Interpretation 11(4), 1–16. https://doi.org/10.1190/int-2023-0016.1.

Palhano, L.C., Nogueira, F.C.C., Marques, F.O., Vasconcelos, D.L., Bezerra, F.H., Souza, J.A.B., Nicchio, M.A., Balsamo, F., 2023. Influence of hydrothermal silicification on the physical properties of a basin-boundary fault affecting arkosic porous sandstones, Rio do Peixe Basin, Brazil . Marine and Petroleum Geology 148, 106062. https://doi.org/10.1016/j.marpetgeo.2022.106062.

Pang, H.-W., Wang, H.-Q., Xiao, Y.-T., Jin, Y., Lu, Y.-H., Fan, Y.-D., Nie, Z., 2024. Machine learning for carbonate formation drilling: Mud loss prediction using seismic attributes and mud loss records. Petroleum Science 21, 1241–1256. https://doi.org/10.1016/j.petsci.2023.10.024.

Pessoa Neto, O.C., Soares, U.M., Silva, J.G.F., Roesner, E.H., Florencio, C.P., Souza, C.A.V., 2007. Potiguar Basin . Petrobras Geosciences Bulletin 15(2), 357-369. Available at: https://bgp.petrobras.com.br/bgp/article/view/326.

Posamentier , H.W., Kolla, V., 2003. Seismic geomorphology and stratigraphy of depositional elements in deep-water settings. J. Sediment. Res. 73 (3), 367–388. https://doi.org/10.1306/111302730367.

Rocha, R.N.R., Nogueira, F.C.C., Pontes, C.C.C., Gomes, T.P.L., Vasconcelos, D.L., Palhano, L.C., Souza, J.A.B., Perez, Y.A.R., Nicchio, M.A., 2025. 3D modeling and fluid flow simulations along fault zone affected by silicification in Rio do Peixe Basin, Brazil. Journal of South American Earth Sciences 161, 105574. https://doi.org/10.1016/j.jsames.2025.105574.

Souza, V.H.P., Bezerra, F.H.R., Vieira, L.C., Cazarin, C.L., Brod, J.A., 2021. Hydrothermal silicification confined to stratigraphic layers: Implications for carbonate reservoirs. *Marine and Petroleum Geology 124, 104818*. https://doi.org/10.1016/j.marpetgeo.2020.104818.

Strugale, M., Lima, B.E.M., Day, C., Omma, J., Rushton, J., Olivito, J.P.R., Bouch, J., Robb, L., Roberts, N., Cartwright, J., 2024. Diagenetic products, settings and evolution of the pre-salt succession in the Northern Campos Basin, Brazil Geol. Soc. London, Spec. Publ. 548. https://doi.org/10.1144/sp548-2023-93.

Yilmaz, O., 2001. Seismic Data Analysis: Processing, Inversion, and Interpretation of Seismic Data . Society of Exploration Geophysicists, Tulsa, OK, 2027 pp. https://doi.org/10.1190/1.9781560801580.

You D., Han, J., Hu, W., Qian, Y., Chen, Q., Xi, B., Ma, H. 2018. Characteristics and formation mechanisms of silicified carbonate reservoirs in well SN4 of the Tarim Basin. Energy Exploration & Exploitation 36, 820-849. https://doi.org/10.1177/0144598718757515.